College of Natural and Computational Science

Department of Chemistry

MSc. Thesis Research on:

Phyto extraction-mediated Synthesis of CuO/ZnO nano composites, from the Leaf Extract of *Phytolacca dodecandra* (Endod) for Antibacterial and Methylene Blue Dye Degradation Applications

A Thesis Submitted to Department of Chemistry Woldia University in Partial Fulfillment of the Requirements for the Degree of Master in Chemistry (Analytical).

By; Habtam Dems Melese

Advisor; Asamene Embiale (PhD)

January, 2025

Woldia, Ethiopia

Woldia University

College of Natural and Computational Sciences

Department of Chemistry

MSc. Thesis Research On: Phyto extraction-mediated Synthesis of CuO/ZnO nano composites from the Leaf Extract of *Phytolacca dodecandra* (Endod) for Antibacterial and Methylene Blue Dye Degradation Applications

A Thesis Submitted to Department of Chemistry Woldia University in Partial Fulfillment of the Requirements for the Degree of Master in Chemistry (Analytical)

Submitted by; Habtam Dems Melese

Name of the Advisor; Asamene Embiale (PhD)

January, 2025

Woldia, Ethiopia

Woldia University

College of Natural and Computational Sciences

Department of chemistry

Thesis Approval Sheet

I, the advisors of the thesis entitled "**Phyto extraction-mediated Synthesis of CuO/ZnO nano composites from the Leaf Extract of *Phytolacca dodecandra* (Endod) for Antibacterial and Methylene Blue Dye Degradation Applications**" developed by Habtam Dems; hereby certify that the recommendation and suggestions made by the board of examiners are appropriately incorporated into the final version of the thesis.

_____	_____	_____
Advisor/Supervisor	Signature	Date

Approval of Board of Reviewers

We, the undersigned, members of the board of examiners the thesis open defense by Habtam Dems Melese have read and evaluated the thesis entitled "**Phyto extraction-mediated Synthesis of CuO/ZnO nano composites from the Leaf Extract of *Phytolacca dodecandra* (Endod) for Antibacterial and Methylene Blue Dye Degradation applications**" and assessed the understanding of the candidate about the proposed research. This is, therefore, to certify that the thesis is accepted for partial fulfillment of the requirement of the degree of Master of Science in Chemistry (Analytical).

_____	_____	_____
Chairperson	Signature	Date
_____	_____	_____
Internal Examiner	Signature	Date
_____	_____	_____
External Examiner	Signature	Date

Final approval and acceptance of the thesis is contingent upon submission of its final copy to the Office of Postgraduate Studies (OPGS) through the Department Graduate Council (DGC) and College Graduate Committee (SGC).

_____	_____	_____
Head, Department	Signature	Date
_____	_____	_____
Collage Dean	Signature	Date
_____	_____	_____
Office of Postgraduate Studies, Dean	Signature	Date

Recommendation

I, the advisor of this thesis, hereby certify that I have read the revised version of the thesis entitled "**Phytoextraction-mediated Synthesis of CuO/ZnO nano composites from the Leaf Extract of *Phytolacca dodecandra* (Endod) for Antibacterial and Methylene Blue Dye Degradation Applications**'' prepared under my guidance by Asamene Embiale (PhD) submitted in partial fulfillment of the requirements for the degree of Master of Science in Chemistry (Analytical). Therefore, I recommend the submission of revised version of the thesis to the department following the applicable procedures.

Major Advisor	Signature	Date

Declaration

I hereby declare that this master thesis entitled "**Phytoextraction-mediated Synthesis of CuO/ZnO nano composites from the Leaf Extract of *Phytolacca dodecandra* (Endod) for Antibacterial and Methylene Blue Dye Degradation Applications**" is my original work. That is, it has not been submitted for the award of any academic degree, diploma or certificate in any other university. All sources of materials that are used for this final thesis have been duly acknowledged through citation.

_____	_____	_____
Name of the student	Signature	Date

Acknowledgement

First, I would like to praise the Almighty God who gives me patience, strength throughout the study period.

I would like to express my deepest gratitude to my research advisor Asamene Embiale (PhD) for his dedicated assistance, consistent guidance, invaluable comments and suggestions and constructive criticism throughout my thesis work.

Special thanks to Woldia University, chemistry Department for giving this chance and providing me the sponsorship.

I am extremely grateful to my best friend Desiew Mekuanint, Adno Asmare and wondefraw Teshome with a deep sense of gratitude that helped me in facilitating conditions and resources throughout my study to complete this research on time.

Table of contents

Recommendation v

Acknowledgement vii

List of Tables xii

List of Figures xiii

List of Abbreviations xv

Abstract xvi

CHAPTER ONE 1

1. Introduction 1

1.1 Back ground of the study 1

1.2 Statement of Problem 4

1.3 Objectives of the study 5

1.3.1 General objective 5

1.3.2 Specific objectives 5

1.4 Significance of the study 6

CHAPTER TWO 7

2. Literature Review 7

2.1 Nanotechnology and Nanoparticle 7

2.2 Types of Nanoparticles 8

2.2.1 Copper oxide Nanoparticle 8

2.2.2 Zinc Nanoparticle 9

2.3 Techniques of Synthesis of CuO, ZnO NPs, and CuO-ZnO NCs 10

2.3.1. Top-down approach 10

2.3.2 Bottom-up approach 10

2.4 Synthesis Methods of CuO/ZnO Nanoparticles 11

2.4.1 Physical methods 11
2.4.2 Chemical methods 11
2.4.3 Green methods 12
2.4.4 Need for Green Synthesis 12
2.5 Synthesis of CuO, ZnO, CuO/ZnO NCs from Plant extracts 13
2.6 Mechanism of CuO, ZnO, CuO/ZnO Nanoparticles Synthesis 13
2.7 Applications of CuO, ZnO NPs and CuO/ZnO NCs 14
2.8 Organic Dye and Its Source 15
2.8.1 Methylene Blue 16
2.9 Medicinal plant (*phytolacca dodecandra*) and It's Use 17
CHAPTER THREE 19
3. Materials and Methods 19
3.1 Chemicals 19
3.2 Apparatus and Instruments 19
3.3 Sample Collection 19
3.4 Extraction of *phytolacca dodecandra* Leaf 20
3.5 Phytochemical Screening 20
3.5.1 Test for Alkaloids 20
3.5.2 Test for Tannins 20
3.5.3 Test for Flavonoids 20
3.5.4 Test for Saponins 21
3.5.5 Test for Phenols 21
3.5.6 Test for Terpenoids 21
3.6 Optimization methods for green synthesis of CuO, ZnO NPs and CuO/ZnO composite 21
3.7 Green synthesis of the CuO, ZnO NPs, and CuO/ZnO NCs 21

3.7.1 Green Synthesis of CuO nanoparticles.....21
3.7.2 Green Synthesis of ZnO Nanoparticles.....22
3.7.3 Synthesis of composite CuO/ZnO NPs.....22
3.8 Characterization of CuO, ZnO NPs, and Composite CuO/ZnO NCs.....23
3.9 Anti-bacterial Activity of the synthesized CuO, ZnO NPs and CuO/ZnO NCs 23
3.10 Photo catalytic activity of synthesized NPs and Nanocomposite.....24
3.10.1 Photo catalytic degradation of MB dye.....24
3.10.2 Reusability of adsorbent (CuO/ZnO NCs).....24
CHAPTER FOUR.....26
4. Results and Discussion 26
4.1 Phytochemical Analysis of the Plant Extracts.....26
4.2 Optimization of Parameters for the Synthesis of CuO, ZnO NPs, and CuO/ZnO NCs.....27
4.2.1 Optimization of Precursor Metal Salt Concentrations 27
4.2.3 Optimization of volume ratio of precursor and plant.....29
4.2.4 Optimization of pH.....29
4.2.5 Optimization of the Ratio of Precursors for Nanocomposite.....29
4.2.6 Optimization of Reaction Time.....29
4.2.7 Optimization of Temperature.....30
4.3 CuO, ZnO and CuO/ZnO NPs.....30
4.4 Characterization of CuO, ZnO NPs and CuO/ZnO NCs.....31
4.4.1 Fourier Transform Infrared (FT-IR) Spectroscopy Analysis.....31
4.4.2. X-Ray Diffraction (XRD) Analysis 34
4.4.3 UV-Vis Analysis 38
4.5 Anti -bacterial Activity of CuO, ZnO NPs and CuO/ZnO NCs 42

4.6 Photocatalytic Activity of Synthesized CuO, ZnO NPs, and CuO/ZnO NCs 46
4.7 Factors affecting Photocatalytic activity of synthesized NPs, and NCs.....47
4.7.1 Effect of pH.....47
4.7.2. Dosage effect of the synthesized NPs and NCs on the Degradation of Dye 48
4.7.3 Effect of initial dye concentration.....49
4.7.4 Effect of contact time 50
4.8 Mechanism of MB dye photo degradation 51
4.9 Recyclability and Reusability of the catalysts.....53
CHAPTER FIVE 55
5. Conclusion and Recommendation 55
5.1. Conclusion.....55
5.2. Recommendation.....56
References.....57
Appendix.....71

List of Tables

Table 1. Dose-relative toxicity of MB for different studies in humans**.**.....16

Table 2. The phytochemical screening of the *phytolacca dodecandra* leaf 27

Table 3. Fourier transforms infrared spectra absorption band (cm^{-1}) for *phytolacca dodecandra* leaf extract, uncalcinate ZnO NPs, CuO NPs, CuO/ZnO (1:2:1) NCs and CuO/ZnO (1:1:1) NCs. 33

Table 4. Evaluation of crystal size D from XRD results of ZnO.....37

Table 5. Evaluation of crystal size D from XRD results of 1:1:1 and 1:2:1CuO composite 37

Table 6. Comparative antibacterial activity of green synthesized CuO NPs, ZnO NPs, 1:1:1 CuO/ZnO, and 1:2:1 CuO/ZnO NCs. 45

Table 7. Optimization of parameters, their amounts for synthesis of nanoparticles and optimum value.....77

Table 8. Optimization parameters and %degradation.....78

List of Figures

Figure 2. Schematic representation of Bottom–up and Top–down techniques 11

Figure 1. Key merits of green synthesis methods 13

Figure 3. Mechanism of CuO, ZnO and CuO/ZnO nanoparticle formation by plant extract 14

Figure 4. *Phytolacca dodecandra* (Endod) Srinika, Monday 01/08/2016.....18

Figure 5. The color change observed when the leaf extract of *phytolacca dodecandra* was tested for the presence of bioactive components (phytochemicals).....26

Figure 6. Synthesized nanoparticles and nanocomposite (A) CuO (B) ZnO (C) CuO/ZnO composite 31

Figure 7. Fourier transforms infrared spectroscopy spectra of (A). a. uncalcinate 1:1:1CuO/ZnO b. uncalcinate ZnO c. uncalcinate CuO d. uncalcinate CuO/ZnO e. *Phytolacca dodecandra* leaf and (B). Calcinated NPs& NCs 34

Figure 8. XRD spectra of ZnO, CuO NPs, CuO-ZnO (1:2:1) and CuO-ZnO (1:1:1) composite 36

Figure 9. UV-Visible spectra of (a) $ZnSO_4.7H_2O$ (b) $CuSO_4 \cdot 5H_2O$ (c) Leaf extract of *phytolacca dodecandera* (d) ZnO (e) CuO NPs (f) (1:1:1) CuO/ZnO NCs (g) (1:2:1) CuO/ZnO NCs. 39

Figure 10. Tauc's plot for optical band gap energy of ZnO NPs, CuO NPs, 1:2:1 CuO/ZnO composite and 1:1:1 CuO/ZnO composite 41

Figure 11. Diagram of Zone of inhibition for microbial activities of plant crude, NPs and NCs with in different concentration (A) represents 25mg/L and (B) represent 50mg/L.....44

Figure 12. Effect of pH on the degradation of MB with in NPs and NCs catalyst.....48

Figure 13. Effect of catalyst concentration (1:2:1 CuO/ZnO NCs, CuO NPs, ZnO NPs and 1:1:1CuO/ZnO NCs) on the degradation of MB 49

Figure 14.Effect of initial dye concentration on the degradation of MB with NPs & NCs catalyst.....50

Figure 15. Effect of contact time on the degradation of MB with in NPs and NCs catalyst.....51

Figure 16. Mechanism of photo degradation of organic dye by ZnO/CuO hybrid nano composite. 53

Figure 17. The degradation efficiency of (1:2:1) ZnO/CuO nano composites over continuous use in three cycles.....54

Figure 18.The UV-Vis spectra of ZnO (A) at pH = 9 formed using 4% of leaf extract and (a) 0.06M (b) 0.08 (c) 0.1M (d) 0.12M of $ZnSO_4.7H_2O$ and CuO (B) at pH = 10 NPs formed using (a) 0.12M (b) 0.08M (c) 0.06M (d) 0.1M of $CuSO_4.5H_2O$.....71

Figure 19. The UV-Vis spectra of NPs formed using 40 mL of 0.1M of Cu and Zn precursor and (a) 3% (b) 4% (c) 5% (d) 6% (e) 7% leaf extract of phytolacca dodecandra pH = 10 and 9 72

Figure 20. The Uv-visible spectra of CuO(A) at pH = 10 and ZnO (B) at pH = 9NPs formed using 4% of leaf powder , 0.1M of Cu and Zn precursor and (a) 2:1 (b) 1:1 (c) 1:2,ratio of leaf extract of phytolacca dodecandra and precursors. 73

Figure 21. The UV-Vis spectra of CuO(A), ZnO(B) NPs and CuO/ZnO(C) NCs formed using 4% of leaf powder, 0.1M of precursor 1:1NPs, and 1:1:1,1:2:1 CuO/ZnO NCs ratio and (a) 12 (b) 11 (c) 10 (d) 8 (e) 9.....74

Figure 22.The UV-Vis spectra of CuO(A) NPs at pH = 10,(1:1)v/v ratio formed using (a) 120min (b) 60min (c) 90min (d) 30min, ZnO(B) NPs at pH = 9,(1:1)v/v ratio formed using (a) 120min (b) 90min (c) 30min (d) 60min and CuO/ZnO(C) at pH = 10, (1:1:1) and (1:2:1)v/v ratio NCs formed using and (a) 30min (b) 120min (c) 60min (d) 90min of 4% leaf extract of *phytolacca dodecandra* and 0.1M precursors.....76

Figure 23. UV–Visible spectra showing the reduction in the intensity of MB solution under sun light irradiation by using (a) 1:2:1CuO/ZnO NCs (b) ZnO NPs (c) 1:1: 1 CuO/ZnO NCs (d) CuO NPs.....80

List of Abbreviations

CuO NPs	Copper Oxide Nanoparticles
ZnO NPs	Zinc oxide nanoparticles
E.Coli	*Escherichia Coli*
FT-IR	Fourier Transform Infrared Spectroscopy
MDR	Multi-Drug Resistances
NP	Nanoparticle
NC	Nanocomposite
UV-Vis	UV-Visible Spectroscopy
XRD	X-Ray Diffraction
MB	Methyl Blue
1:2:1 CuO/ZnO v/v	30ml $ZnSO_4.7H_2O$ + 60ml $CuSO_4.5H_2O$ + 30ml leaf extract
1:1:1 CuO/ZnO v/v	30ml $ZnSO_4.7H_2O$ + 30ml $CuSO_4.5H_2O$ + 30ml leaf extract

Abstract

The syntheses of metal oxide nanocomposite by using the green method has gotten special consideration due to a cheaper, ecofriendly and good catalytic, electric, optical, photonic, and antibacterial activity. The current study is focused on the synthesis of CuO/ZnO nano composites (NCs) via aqueous Phytolacca dodecandra leaf extract with the corresponding precursors $ZnSO_4.7H_2O$, and $CuSO_4.5H_2O$. XRD, FTIR and UV-Visible (UV-Vis) spectroscopy have been used for characterization of the synthesized NCs. The crystalline size of the synthesized CuO, ZnO NPs, (1:1:1) CuO/ZnO and (1:2:1) CuO/ZnO nano composites were found to be 19.9, 17.1, 27.6 and 30.5nm respectively. The UV-Visible (UV-Vis) absorption band showed that surface plasmon resonance of CuO, ZnO, (1:1:1) CuO/ZnO and1:2:1(CuO/ZnO) were 401, 375,411,418 nm respectively. The energy band gap for the synthesized NPs and NCs were also calculated and found to be 2.83, 2.6, 2.4 and 2.3 eV for CuO, ZnO, (1:1:1v/v)CuO/ZnO and (1:2:1v/v)CuO/ZnO respectively. The qualitative phytochemical analysis confirmed the presence of secondary metabolites in the extract. Methyl blue organic contaminants (MB) have been removed effectively from wastewater by photo degradation using synthesized NCs. Thus, a high photo-degradation efficacy was achieved by the nanocomposite formulation, which 81.5% of organic MB dye was removed after120min. The synthesized (1:2:1v/v) CuO/ZnO composite result confirmed highest inhibition against salmonella and Escherichia coli ATCC was, 20.33±0.5 mm and 19.66±0.5 mm, respectively. In general, the green synthesized nano composites showed an effective antibacterial activity and removal of MB organic dye.

Keywords: Green synthesis, *phytolacca dodecandra leaf,* CuO NPs, ZnO NPs, CuO/ZnO NCs, MB dye degradation, Antibacterial activity

CHAPTER ONE

1. Introduction

1.1 Back ground of the study

The risks of environmental pollution and bacterial resistance to antibiotics are the major concern of world population [1]. Microorganism infections have gained significant attention due to the serious health hazards they pose. Hence, to overcome such problems, antimicrobial drug use, both by humans and animals, is on the rise. However antibiotic resistance in microbsis one of the biggest issues facing humanity today, according to the WHO. Another factor contributing to the growing problem of bacterial resistance is the incorrect prescription of antimicrobial therapy. Physician overuse of numerous popular antimicrobial medicines may arise from the selection of drugs based on a combination of low cost and low toxicity. Bacterial resistance can result from either a natural or acquired process. Thus, the four primary types of processes underlying antimicrobial resistance: (1) limiting uptake of a drug, (2) modifying a drug target, (3) inactivating a drug; (4) active drug efflux [2-4]. On the other hand, the environmental pollution is increasing due to rapid human population, which industrial operations, agricultural practice, transportation facilities and domestic activities are the major contributing factors identified in recent decades. Dyes, such as methylene blue (MB), are widely used in various industries including food, paper, rubber, printing, cosmetics, textile, plastic, and concrete. When these dyes are released into water bodies through industrial effluents, they can contaminate the water, posing a threat to both humans and aquatic life [5, 6].

For instance, acute MB exposure will result in a number of physiological reactions, including elevated heart rate, vomiting, and dangerous diseases such cyanosis, dyspnoea, and tachycardia [7].Consequently, removal of MB dye is highly recommended that degradation methods using photocatalysts are an excellent way to eliminate hazardous or cancer-causing dyes including MB [8]. Photocatalysis involves the direct or indirect absorption of light, visible or UV photons, by a semiconductor that helps eliminate pollutants by converting solar radiation into hydroxyl radicals,

followed by oxidize chemical pollutants. The presence of a catalyst accelerates a photo reaction in photocatalysis, enhancing the oxidation process [9].

In recent years, photocatalysis using nanostructured materials has made significant progress in the fields of drug degradation, dye degradation, and water splitting. Photocatalysis, particularly using metal oxide nanostructures such as ZnO, TiO_2, WO_3, CuO, Cu_2O, and Fe_2O_3, shows promise in effectively removing organic pollutants from wastewater due to the special qualities and adaptability of these metal oxides [10]. Inorganic metal oxide nanoparticles are considered intriguing due to their safety, effectiveness in germ-killing and chemical stability. Metal oxide nanoparticles are widely used in various industries, including pharmaceuticals, environmental, industrial application (electronics, superconductor) and are highly important in the field of nanotechnology. They are used as antibacterial medications, fillers, disinfectants, and catalysts. For example zinc oxide nanoparticles (ZnO), which are n-type semiconductors, are a unique material with specific electrical conductivity [11].

Conversely, copper oxide nanoparticles (CuO) are considered to be another type of widely used p-type semiconductor. In general ZnO and CuO NPs are environmentally friendly, chemically stable, and have low band gap energy. They are known for their excellent chemical, physical, and mechanical properties, making them widely used. Some of these properties include low melting temperature, large surface area, structural stability, high diffusion, and high surface energy [12].

CuO, ZnO NPs and CuO-ZnO NCs can be synthesized using various techniques such as physical, green, and chemical procedures. One of the most commonly used methods is the green synthesis approach, which involves using plants to create nanoparticles. This innovative method offers advantages such as low cost, environmental friendliness, and ease of scaling up for large-scale production. Additionally, it eliminates the need for hazardous chemicals or high temperatures, pressures, or energies. Despite fungi and bacteria can also be used for nanoparticle synthesis, using plant leaf extract is a more cost-effective and simpler alternative that doesn't require specific isolation and culture preparation methods [13, 14].

The addition of CuO to ZnO could form the CuO/ZnO NCs, which increases particle size and decreases the band gap energy. The ability of the materials to transfer charge and absorb light more effectively is due to the properties of NCs rather than just using

the individual NPs. They have some important characteristics: they are very stable when exposed to heat, and they have a large surface area. This helps them react better because they have more active sites on their surface and they work more effectively [15, 16].

The synthesis of CuO−ZnO NCs was reported using extracts of plants like *Clerodendrum infortunatum* [17], *Vaccinium arctostaphylos* L. [18], *Ginkgo biloba* [19] and *Verbascum sinaiticum* [20] that have been showed a range of different characteristics. To our knowledge, there has not yet been a publication on CuO−ZnO NC catalyst synthesized using *phytolacca dodecandra*.

Phytolacca dodecandra is one of the traditional medicine plant it is used to treat many infectious diarrhea, intestinal infection, skin infection, dysmenorrhea in human and animal, contraceptives [21]. Many people in North Wollo have been used *phytolacca dodecandra* to treat various illnesses such as gout, measles, and rabies. Therefore, researching the plant's antimicrobial properties could greatly benefit society.

The main goals of this study were to synthesis CuO, ZnO, and CuO/ZnO NCs using *phytolacca dodecandra* leaf extract in a cost-effective and environmentally friendly way, and to assess their antibacterial activity and ability to degrade MB.

1.2 Statement of Problem

Nanotechnology utilizes tiny particles known as nanoparticles, which are widely employed in various fields of research. There is a wide range of elemental nanoparticles, such as Cu, Au, Ag, Ti, Zn, Si, and Pd. Zinc and copper, in particular, exhibit superior photocatalytic and antimicrobial activity, significant biocompatibility, non-toxic catalyst properties, and efficient heat and electricity conductivity. CuO nanoparticles are highly reactive and readily interact with other materials due to their high surface-to-volume ratio [22]. CuO/ZnO is receiving increasing attention in the field of metal oxide nano composites due to its availability, affordability, and lack of toxicity. It is more abundant, has better electrical and piezoelectric properties, a high energy density, delays electron-hole recombination, and exhibits stronger photocatalytic and antibacterial activity. ZnO can be modified with transition metals (CuO) to enhance its performance. This is because it is a p-type semiconductor that can act as a photo catalyst when exposed to sunlight, owing to its low band gap [23].

Upon learning that there are still undiscovered multi-drug resistant (MDR) bacterial strains, an increase in organic dye (MB) contamination of water, and insufficient knowledge among people about proper plant medicine dosage, it became clear that this is a major public health concern. To address this issue, effective, commercially feasible, and widely applicable novel medications were developed, along with a good catalytic green synthesis using plant extracts to synthesize CuO/ZnO NCs.

To the best of my knowledge, no literature has described the synthesis of CuO/ZnO NCs utilizing *phytolacca dodecandra* leaf aqueous extract and tested its antibacterial activity and MB dye degradation.

1.3 Objectives of the study

1.3.1 General objective

The main objective of this study was to synthesize and characterize CuO/ZnO composite nanoparticles using an aqueous leaf extract of *phytolacca dodecandra* for antibacterial testing and degradation of MB dye.

1.3.2 Specific objectives

The specific objectives of this study:

- To identify phytochemicals (phenols, alkaloids, tannins, saponins, flavonoids, terpenes) from leaf extract of *phytolacca dodecandra*.
- To optimize the effect of precursor concentration, plant concentration, pH, temperature, contact time on the synthesis of CuO, ZnO NPs and CuO/ZnO NCs.
- To synthesize CuO, ZnO NPs and CuO/ZnO NCs using leaf extract of *phytolacca dodecandra*.
- To characterize the synthesized CuO, ZnO NPs and CuO/ZnO NCs using UV-Vis, FTIR and XRD.
- To evaluate the anti-bacterial activities and MB dye degradation of crude plant extract and synthesized nanoparticles.
- To optimize the effect of pH, synthesized NPs dose, contact time, concentration of adsorbate on degradation of methylene blue dye.

1.4 Significance of the study

The ultimate goals of this work are to enhance social well-being and environmental protection. The most practical, easy, and environmentally responsible method for synthesizing nanoparticles is the one that reduces the negative consequences of chemical and physical procedures by not using poisonous chemicals, producing dangerous byproducts, or endangering the environment or human health.

Hence, the study developed a cost-effective and environmentally friendly method for synthesizing CuO, ZnO, and CuO/ZnO nano-composites using *phytolacca dodecandra* leaf. The approach was found to be more effective in degrading organic dyes (MB) in wastewater compared to other affordable or straightforward methods.
Moreover, result of this work can used to address the public health issue of drug resistance caused by disease-causing microbes. The study will also be used for as a further baseline for similar studies conducted in the area.

CHAPTER TWO

2. Literature Review

2.1 Nanotechnology and Nanoparticle

Nanotechnology refers to the design, synthesis, and use of materials and devices at the nanoscale, which involves manipulating matter at the atomic and molecular level. This field takes advantage of unique mechanical, electrical, chemical, and physical properties that arise from the nanoscale structure of matter. Nanotechnology has diverse applications in areas such as medicine, including treatment of diseases and drug delivery, as well as in electronics, catalysis, and materials science. Materials and systems at the nanoscale exhibit novel and significantly altered physical, chemical, and biological characteristics, leading to the term nanotechnology [24, 25].

The term “nanoparticles” is used to describe a particle with size in the range of 1nm-100nm, at least in one of the three possible dimensions. In this size range, the physical, chemical and biological properties of the nanoparticles changes in fundamental ways from the properties of both individual atoms/molecules and of the corresponding bulk materials [26]. NPs are not simple molecules itself and therefore composed of three layers.

a) The surface layer, which may be functionalized with a variety of small molecules, metal ions, surfactants and polymers.

b) The shell layer, which is chemically different material from the core in all aspects

c) The core, which is essentially the central portion of the NP and usually refers the NP itself [27].

Nanomaterials are made up of small particles with a large specific surface area, unlike materials with an undefined particle size. This gives them unique properties such as unexpected surface area, volume, quantum size, and macro tunneling effects. Due to these characteristics, nanomaterials display distinctive optical, mechanical, catalytic, and biological properties, making them potentially useful in a wide range of applications [28, 29]. Nanoparticles (NPs) have unique thermal, electric, chemical, magnetic, optical, and physical properties, unlike their bulk materials due to possessing quantum effects and high surface-to-volume ratio. Nanoparticles have a wide range of application like electronic, magnetic, optical, cosmetics, sunscreen

lotions, bio molecule detection, diagnostics and drugs. They are also extensively used in the formulation of health care products [30].

Nanoparticle synthesis is currently one of the most captivating scientific fields. There is increasing interest in producing nanoparticles using environmentally friendly methods. This involves creating nanoparticles using materials like plant extracts, bacteria, fungi, and algae, which offer advantages over traditional processes that use chemical agents associated with environmental toxicity [31, 32].

The chemical and physical methods for synthesizing nanoparticles are time-consuming, expensive, and produce toxic waste due to the use of chemical agents. The size, stability, and properties of the nanoparticles are significantly influenced by various factors during the synthesis process, such as concentration, temperature, and the interactions between the metal ion precursors and the reducing agents. Biological synthesis of nanoparticles from plant extracts is a promising alternative to reduce toxicity, cost, and time. Biologically synthesized nanoparticles are considered to be biocompatible, non-toxic, and can be used as drug carriers and fillers in medical materials [33, 34].

2.2 Types of Nanoparticles

There are generally two types of nanoparticles: inorganic and organic. Inorganic nanoparticles are typically made of metal or metal oxides such as Ag, Fe_3O_4, TiO_2, CuO, and ZnO. They are preferred over existing chemical imaging pharmacological agents and pharmaceuticals due to their size features and advantages. Organic nanoparticles are mostly composed of lipids or polymers and have a diameter ranging from 1 nm to 100 nm. The bactericidal effect of inorganic nanoparticles is attributed to their unique size, which is smaller than the bacteria's pore size, allowing them to pass through cell membranes easily. Due to their availability, functionality, compatibility, and capacity for targeted and controlled drug release, inorganic nanomaterials are extensively used for cellular delivery [35, 36].

2.2.1 Copper oxide Nanoparticle

CuO nanoparticles have a wide range of potential applications in various industries, such as photovoltaic, gas sensors, antimicrobials, batteries, catalysis, high temperature superconductors, solar energy conversion, and field emission emitters. Currently,

several physical and chemical methods are used to produce them, including microwave irradiation, hydrothermal, sonochemical, thermal decomposition, and rapid precipitation. However, these methods have their own limitations, such as the need for chemical reagents, labor intensiveness, cost, and the presence of hazardous substances. Copper oxide (CuO) nanoparticles are considered to be a safe inorganic material and have been extensively studied due to their potential applications in various fields such as antimicrobial, gas sensors, catalysis, batteries, high temperature superconductors, solar energy conversion, photovoltaic devices, and field emission emitters. Currently, various physical and chemical methods such as hydrothermal, sonochemical, sol-gel, thermal decomposition, colloidal thermal synthesis, microwave irradiation, solution method, and quick precipitation method are used for the preparation of CuO nanoparticles with desired size and morphologies. However, these methods have their drawbacks including toxicity, high cost, the use of hazardous materials, chemical reagents, and labor intensiveness [37, 38].

2.2.2 Zinc Nanoparticle

Zinc oxide nanoparticles (ZnO NPs) are highly advantageous due to their rapid creation, lack of toxicity, biocompatibility, antibacterial and photocatalytic activities. These nanoparticles are manufactured using plant extracts as biological reducing and stabilizing agents, as well as various microbes and fungi. ZnO NPs find wide applications in electrochemistry, catalysis, medical devices, cleaning agents, textile industries, food preservation, and pollutant sensor , owing to their high surface area-to-volume ratio [39].ZnO is n-type semiconductor with a wide band gap eV that is considered a propitious photocatalysts due to its high chemical stability and excellent photocatalytic activity. The impressive photocatalytic properties of ZnO are because of its exciting physical and chemical characteristics such as its high electro- chemical stability, super oxidative capability, and low toxicity. Shortcomings of ZnO such as wide band gap confine its practical application in the field of water purification and restrict its optical absorption in UV region of the solar spectrum Furthermore, in the aqueous solution ZnO exhibits deprived photo-stability and poor photocatalytic efficiency due to fast rate of electrons–holes recombination of ZnO [40].

2.3 Techniques of Synthesis of CuO, ZnO NPs, and CuO-ZnO NCs

Green synthesis of nanoparticles is categorized in to classes, namely “top-down” and “bottom-up” based on the way of nanoparticle formation [41].

2.3.1. Top-down approach

When starting with bulk materials of the same composition that will be synthesized and applying energy to break down the larger materials into tiny fragments, the goal is to reduce the size of the structure to the nanoscale. However, this approach has a drawback in that it results in particles with a wide size distribution [42, 43].

2.3.2 Bottom-up approach

The process involves creating larger nanostructures from smaller atoms and molecules. An alternative approach that could reduce waste and be more beneficial for producing nanoparticles is the bottom-up method. This method involves building a substance from the ground up, atom by atom, molecule by molecule, or cluster by cluster. It starts with a simple metal salt, gradually transforming it from ions to elemental atoms, and eventually forming nanoparticle-sized particles. Many of these methods are still in the early stages of development or are just beginning to be used in the commercial manufacturing of nano powder [44, 45].Throughout the further progression, the physical forces working at nanoscale combined simple units into larger stable structures [46]. The synthesis process is illustrated in **figure 1.**

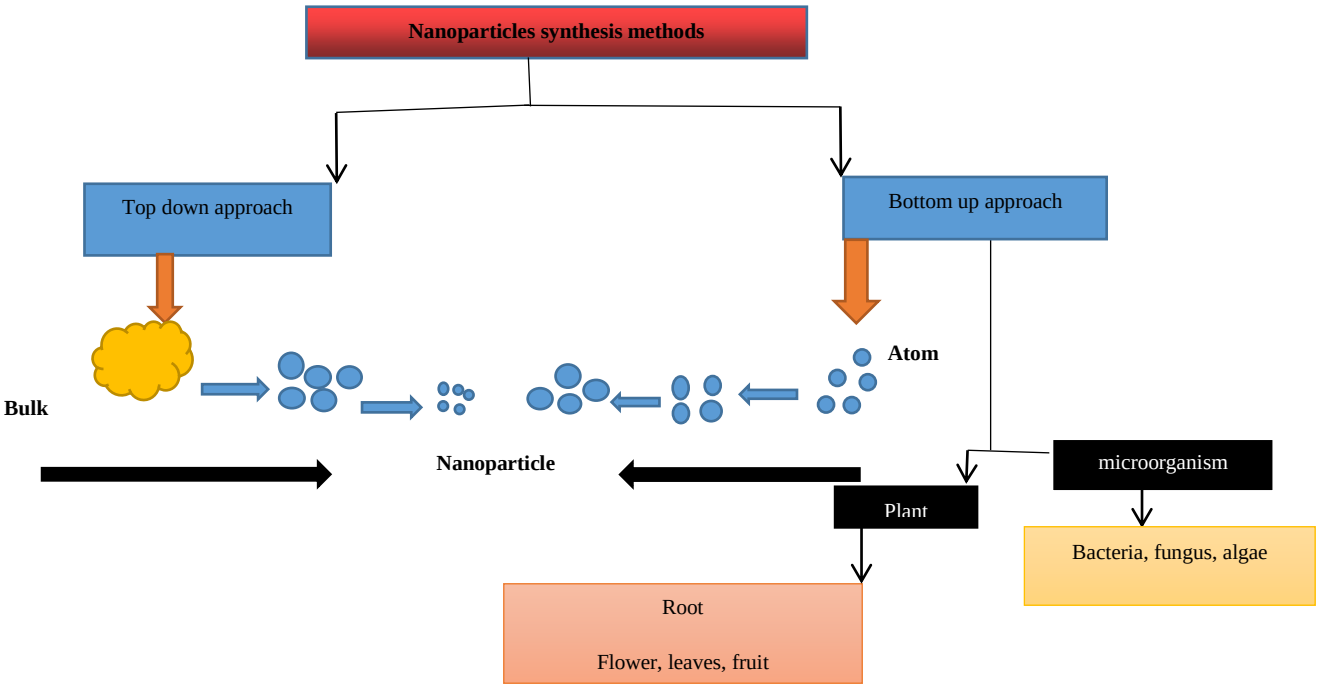

Figure 2. Schematic representation of Bottom–up and Top–down techniques [41].

These two techniques contain three sub methods to synthesis CuO, ZnO, CuO/ZnO NCs, but the best one is green methods.

2.4 Synthesis Methods of CuO/ZnO Nanoparticles

2.4.1 Physical methods

Physical methods for producing nanoparticles include lithographic processes, sputter deposition, layer-by-layer growth, molecular beam epistaxis, diffusion flame synthesis of nanoparticles, plasma arcing, ball milling, thermal evaporation, spray pyrolysis, and ultrathin films. However, these methods have limitations in synthesis, high energy consumption requirements, and can be very expensive [47].

This approach are not use of solvent contamination in the prepared thin films and the uniformity of nanoparticles distribution are advantages than chemical approach [48].

2.4.2 Chemical methods

The widely used chemical approaches are based on chemical solutions, including chemical reduction, irradiation, electrolysis, pyrolysis, and sol-gel processing. While these methods are low-cost, they require the use of toxic solvents and result in chemical contamination with the generation of toxic by-products. It is important to use protective agents to stabilize dispersive nanoparticles during the course of metal

nanoparticle preparation and to protect the nanoparticles that can be absorbed on or bind onto the nanoparticle surface, thus avoiding their agglomeration [49, 50].

2.4.3 Green methods

The goals of green synthesis of nanomaterials are twofold: (1) creating nanomaterials to address environmental issues by preventing harm from known pollutants or incorporating nanomaterials into environmental technologies to clean up polluted environments, and (2) producing nanomaterials that can minimize the harms of human activities to human health or the environment. Green methods involve using eco-friendly resources such as plants, bacteria, fungi, algae, and enzymes. This approach is advantageous over chemical and physical methods as it is safe, simple, cost-effective, relatively reproducible, and often results in more stable materials [51, 52].

This method provides a safer alternative for creating nanoparticles with the necessary chemical and physical characteristics. The size and shape of the nanoparticles generated are influenced by the type of green synthesis employed, the quantity of extract used, and the experimental settings. Plant extracts contain secondary metabolites such as polyphenols, alkaloids, flavonoids, and terpenoids, as well as enzymes in microorganisms, which act as both reducing and capping agents, leading to the formation of stabilized nanoparticles without the need for capping moieties [53]. However, microbe-based green synthesis is unattractive due to the requirement for aseptic culturing and its high cost for commercial nanoparticle production. As a result, an increasing number of researchers have focused on the synthesis of CuO-ZnO nanoparticles [54, 55].Due to their wide-ranging applications in various cutting-edge scientific fields [56].

2.4.4 Need for Green Synthesis

The main process in the green synthesis of nanoparticles is reduction/oxidation, which is a bottom-up approach. The cost of the physical and chemical processes has led to an increased demand for nanoparticle biogenesis. Chemical synthesis methods often lead to the surface absorption of hazardous chemicals, which could have adverse effects on medical applications. However, in the case of nanoparticles biosynthesized using the green synthesis method, this is not an issue [57].With their antioxidant or reducing properties they are usually responsible for the reduction of metal compounds

into their respective nanoparticles. Green synthesis provides advancement over chemical and physical method [58].

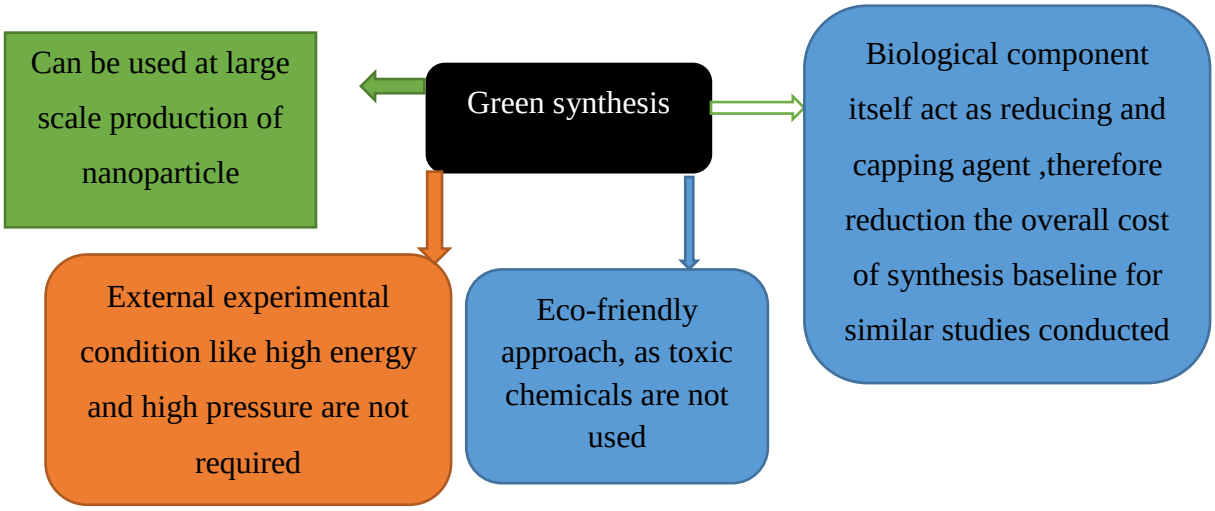

Figure 1. Key merits of green synthesis methods [59]

2.5 Synthesis of CuO, ZnO, CuO/ZnO NCs from Plant extracts

One of the earliest methods of producing nanoparticles is using plants as a source. However, the polydispersity of the nanoparticles produced remains a difficulty, despite the advantages of biological synthesis. Using different plants and their extracts to synthesize nanoparticles can have advantages over other biological synthesis methods that require laborious steps to maintain microbial cultures. The most extensively used technique for producing green, eco-friendly CuO/ZnO nanoparticles is the synthesis of the particles using plant extracts. This method also has the unique benefit that plants are widely available, considerably safer to handle, and widely dispersed [60, 61].

2.6 Mechanism of CuO, ZnO, CuO/ZnO Nanoparticles Synthesis

Plant extracts contain secondary metabolites and phytochemicals that act as stabilizing and reducing agents during the production of metal nanoparticles. These compounds can be utilized as bio resources to create CuO, ZnO, and CuO/ZnO NPs. Phenols and flavonoids, which are the most important phytochemicals in plants, are found in various plant parts such as shoots, leaves, stems, flowers, roots, and fruits. These phenolic molecules contain both hydroxyl and ketone groups [62].

The nanoparticles produced through this eco-friendly process demonstrated increased stability and were capable of adsorbing phytochemicals on their surface to enhance

their reaction rate. Furthermore, the nanoparticles were able to prevent agglomeration and deformation. To create ZnO, CuO, and CuO/ZnO nanoparticles, a specific amount of precursor is combined with a known quantity of plant extract. The mixture is then heated to a predetermined temperature and constantly stirred for a set amount of time [63, 64].

The reducing agent in the plant extract could be one of the biomolecules found there, or it could be one of the same molecules that serve as the capping and reducing agents. Since different plant extracts include various phytoconstituents, different plant species have diverse methods for forming nanoparticles, the specifics of which have not yet been thoroughly understood [65].

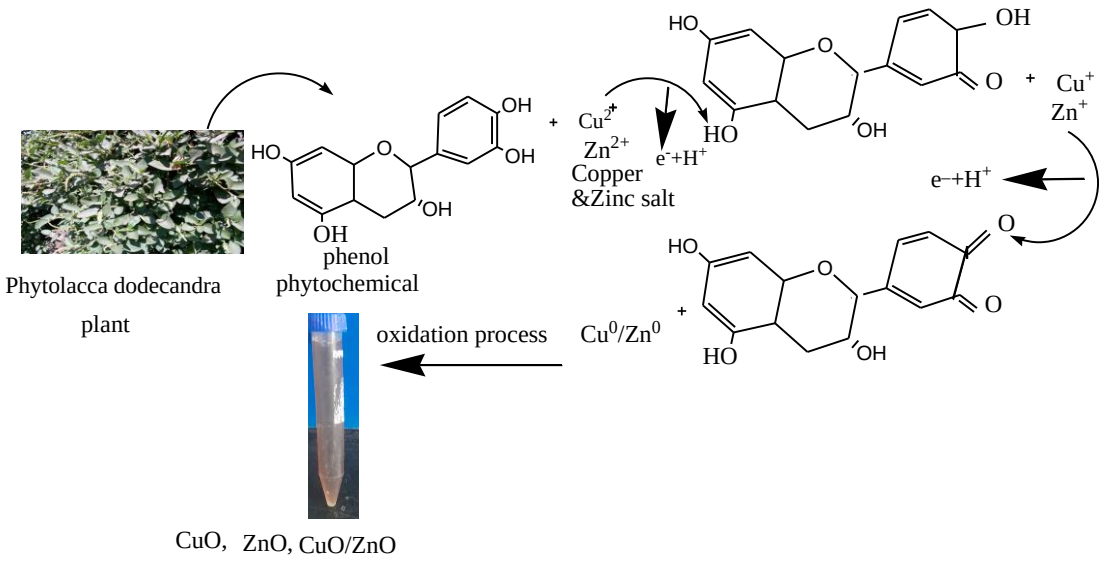

Figure 3. Mechanism of CuO, ZnO and CuO/ZnO nanoparticle formation by plant extract [66]

2.7 Applications of CuO, ZnO NPs and CuO/ZnO NCs

Due to their incredibly small size and high surface-to-volume ratio, nanoparticles have different properties compared to bulk materials with the same chemical composition. These properties include mechanical, biological, and steric qualities, catalytic activity, thermal and electrical conductivity, optical absorption, and melting point, making nanoparticles of great interest. CuO and ZnO nanoparticles are particularly interesting in demand for their potential applications in various biomedical sectors, including as antimicrobials, antioxidants, imaging agents, and for drug administration. Metal oxide nanoparticles are effective photocatalysts, with

CuO/ZnO nano composites exhibiting unique properties in photocatalysis when exposed to sunlight [67, 68].

Compared to ZnO and CuO nanoparticles alone, the synthesized CuO/ZnO nanocomposite is more stable. The materials for the ZnO and CuO/ZnO nanocomposite (NCs) were synthesized using the energy-efficient and speedy solution combustion synthesis (SCS) process. By increasing the charge and absorption capabilities of the materials, the nanocomposite outperforms employing individual nanoparticles in terms of light transfer. The composition of two metal oxides results in a mixture that has several significant properties, including a huge surface area and extreme heat stability. Because they have more active areas on their surface and are more efficient, this aids in their ability to react [69].

2.8 Organic Dye and Its Source

Dyes are colored compounds that are extensively used in textiles, printing, rubber, cosmetics, plastics, and leather industries to add color to their products, resulting in the generation of a large amount of colored wastewater. Dyes are mainly classified into anionic, cationic, and non-ionic types. Among all industries using dyes, textile industries are the largest consumers of dyes for coloring fibers [70, 71].

Chemical substances known as dyes adhere to textiles or surface shells to add color. Environmental managers encounter a significant challenge when it comes to treating water effluent from the textile and manufacturing industries, as dyes are soluble in water and create vibrant colors in acidic water. It is projected that the textile and manufacturing sectors use over 10,000 commercially available dyes globally. Annually, the textile industry consumes over 1000 tons of dyes, with approximately 10-15% of these dyes being released into waste streams as effluents during the dyeing processes [72, 73].

Various production facilities, such as those in the food, leather, paper, cosmetics, pharmaceutical, dyeing, printing, and textile industries, discharge dye into water bodies. This contributes to water pollution as these dyes are extremely toxic and can even cause cancer in mammals and microorganisms. Since these dyes are stable to light and non-biodegradable, they are difficult to remove from industrial effluent and resistant to aerobic digestion. Therefore, it is important to collect and treat these dyes before they are released into water bodies [71, 74].

2.8.1 Methylene Blue

The production operations of the paint, leather, paper, and cosmetics industries release industrial effluents that contain a significant amount of poisonous aromatic dyes, particularly thiazine cationic dyes such as methylene blue (MB). MB ($C_{16}H_{18}C_lN_3S$) has beneficial applications in various scientific fields. However, due to its solubility in water, the dye poses a risk to humans, other living organisms, and the environment. Additionally, MB dye has the potential to be harmful to human health and can cause persistent poisoning, particularly to the central nervous system. The effluents and wastes generated by the cosmetics, textiles, paper, leather, and paint industries are highly colored, contain salt concentrations in high quantities, and have high biological oxygen demand as well as chemical oxygen demand values [75, 76].

Table 1. Dose-relative toxicity of MB for different studies in humans**.**

Doses(mg/kg)	**Symptoms**
2–5	Hemolytic anemia, fever, methemoglobinemia, nausea, vomiting, chest pain, dyspnea, and hypertension
>5	Fatal serotonin toxicity
20–80	Refractory hypotension, reduced renal blood flow, fainting, and dermal discoloratin

Due to its resistive nature, MB is difficult to remove from wastewater using standard treatment methods. When exposed to photolysis or conventional water treatment under typical environmental conditions, its complex, highly resistant, and chemically stable structure prevents it from breaking down into less harmful compounds. It is composed of atoms of functional groups containing nitrogen, aromatic rings, and conjugated double bonds, which give it its intense blue color. This type of dye reduces the amount of light that enters the water, affects photosynthesis, and promotes the growth of harmful bacteria, impacting both human health and aquatic life. Innovative and specialized treatment strategies such as photocatalysis and advanced oxidation processes are typically required to effectively remove MB from water systems [77, 78].

2.9 Medicinal plant (*phytolacca dodecandra*) and It's Use

A medicinal plant is any plant that contains substances in one or more of its organs that can be used for therapeutic purposes or as precursors for the synthesis of useful drugs. This distinction allows us to differentiate between medicinal plants whose therapeutic properties and constituents have been scientifically established and plants that are considered medicinal but have not yet been thoroughly studied scientifically [79]. A number of plants have been used in traditional medicine for many years [80].

According to estimates from the World Health Organization (WHO), 80% of people in underdeveloped countries use traditional herbal treatments. Due to their effectiveness, cultural significance, and availability, traditional medicines provide a low-cost and alternative source of primary healthcare in underdeveloped nations. Ethiopia, with its diverse climate zones, is home to 6,000 different species of vascular plants, many of which are used for medicinal purposes [81]. The indigenous knowledge on medicinal plants transfers from generation to generation orally. Various parts of the plant are widely used in traditional medicine in Africa to treat a wide range of ailments, presence of a range of medically active compounds. The leaves, fruits and roots contain numerous saponins triterpenoid, alkaloids, phenols, flavonoids and glycosides [82].

The *phytolacca dodecandra*, also known as "Endod" or "gobo berry," is a woody plant found in South Africa, Madagascar, Sub-Saharan Africa, South America, and Asia. It belongs to the Phytolaccaceae family and can grow up to nine meters in length, with long, dangling branches. The leaves are thick, juicy, shiny, oval-shaped, and can grow up to 25 cm in length, with a pink stalk and midrib. The flowers have many stamens on a fleshy disc, five sepals but no petals, and emit a strong perfume. They are cream-green in color and grow on spikes up to 40 cm, often with opposite leaves. The fruit is a rounded, soft fruit with a 7 mm seed in each part, and turns orange-red when ripe [83]. Ethiopians are familiar with *phytolacca dodecandra*, which is widely used for soap production. Scientist Aklilu Lema of Ethiopia found that it was effective in controlling schistosomiasis and deadly to snails. Other than soap, people in the area use Endod for various purposes. Endod is also used to treat digestive issues such as diarrhea, stomach pain, and oedema [84].

The leaves, whether fresh, dried, or powdered, are used to treat wounds and skin conditions such as vitiligo, ringworm, scabies, eczema, psoriasis, and leprosy. Many people use the fruit infusion or root decoction to induce abortions, treat rabies, malaria, bilharzia, sore throats, and other respiratory issues, rheumatic pain, and jaundice, among other conditions [85].

Figure 4. *Phytolacca dodecandra* (Endod) Srinika, Monday 01/08/2016

CHAPTER THREE

3. Materials and Methods

3.1 Chemicals

Copper (II) sulphate pentahydrated ($CuSO_4 \cdot 5H_2O$, 98.5%, Maharashtra India), Zinc sulphate heptahydrate ($ZnSO_4.7H_2O$, 99.5%, Maharashtra India), ferric chloride ($FeCl_3$, 98%, Maharashtra India), Hydrochloric acid (HCl, 35.4%, Maharashtra India), sulfuric acid (H_2SO_4, 98%, India), potassium iodide (KI, 99.71%, India) chloroform (99.9%, India) methyl blue ($C_{16}H_{18}C_lN_3S$) was from AbroExport-133001,India, iodine (I_2, 99.8%, Mumbal 400021 India), acetic acid anhydride (99.5%, UDYOG-121001,india), ethanol (C_2H_5OH, 96%, Addis Abeba Ethiopia), sodium hydroxide (NaOH, 99.8%,Norbright China), German; agar Hilton Muller was obtained from Oxoid CM, UK; and distilled water was used for this study. All these chemicals and reagents are analytical grade and used without any further purification. Moreover, the currently working anti-bacterial drug, Gentamicin, was used as positive control for anti-bacterial study.

3.2 Apparatus and Instruments

The instruments used in this study includes glassware, magnetic stirrer with heating (MS7-H550-S), calcination furnace (FCD3000), Uv-Vis spectrophotometer (Uv 9000Uv/Vis spectrophotometer) was obtained from SHANGHAIME ASHINSTRUMENTS CO..LTD, Rotary evaporator (RE100-pro LCD Digital Rotary Evaporator was from Shunyi District, Beijing, 101318, China), oven, pH meter (AD 8000) was from ROMANIA-Lot-13344, centrifuge (12HoleIndia), Analytical balance (FA2104), water distiller (water still-Lasany LPH-4) burette, spatula, volumetric flask, enlimenary flak, test tube, measuring cylinder, funnel, filter paper, FT-IR (Jasco-FT/IR-6600A), and XRD (XRD-7000X-RAY DIFFRATOMETER) were used. All the glassware was washed with distilled water and drying in oven.

3.3 Sample Collection

Fresh *phytolacca dodecandra* leaves were collected from Woldia specifically Srinika using a clean polyethylene plastic bag during chilly or morning time in January and April 2016E.C. Simple random sampling technique approach was implemented for

the sampling. Once, the sampling of the leaves has been over, the collected samples were transported to Woldia university chemistry laboratory.

3.4 Extraction of *phytolacca dodecandra* Leaf

The fresh leaves of *phytolacca dodecandra* was washed gently with tap water and distilled water to removed dust particles and were allowed to dry in a shade place at room temperature for 15 days and then the dried leaf was pulverized using grander, which is ready for extraction. 4g of the leaves powder was taken into 250 mL enlimenary flak followed by adding of 100 mL of distilled water, then the mixture was stirred at1200 rpm, 80 °C for 30 min using a magnetic stirrer heating mantel. Then, the suspension was allowed to cool down at room temperature and was then filtered using 90 mm watt man filter paper. The suspension of leaf extract was then stored at 4°C refrigerator to prevent moisture effect [13].

3.5 Phytochemical Screening

The preliminary qualitative phytochemical analysis of the plant extracts of *phytolacca dodecandra* will performed to screen for the presence of bio-active components in the leaf extract [86].

3.5.1 Test for Alkaloids

***Wagner's Test*:** 1.2 g of iodine and 2 mL of H_2SO_4 was mixed and diluted to 100 mL solution. 4 mL of the leaf extract was acidified by adding 1.5% (v/v) of HCl and then few drops of Wagner's reagent (1g of I_2 + 3g of KI mixed with100ml of distilled water) were added. Yellow precipitate was assessed to confirm the presence of alkaloids [87].

3.5.2 Test for Tannins

Ferric Chloride Test: 1ml leaf extract and 1mLferric chloride solution was mixed and stirred and allow diffusing for a few minutes. Brownish green was observed [86].

3.5.3 Test for Flavonoids

2 mL leaf extract with 8 drops NaOH solution was mixed and the mixture was shaking. A brownish precipitate was observed. It indicate the presence of flavonoid [49].

3.5.4 Test for Saponins

Foam Test: 3 ml of distilled water with 2ml leaf extract was mixed and shake vigorously for about 1 min. After shaking foam was observed it indicate the presence of saponins [88, 89].

3.5.5 Test for Phenols

2 ml of leaf extract and 2 ml of distilled water followed by a few drops of 10% ferric chloride solution was mixed bluish black color was observed that indicate the presence phenols [90].

3.5.6 Test for Terpenoids

2 mL of leaf extract was mixed with 2 mL of chloroform and 3 mL of concentrated H_2SO_4 was added carefully to form a layer. Reddish-brown coloration of the interface indicates the presence of terpenes [91].

3.6 Optimization methods for green synthesis of CuO, ZnO NPs and CuO/ZnO composite.

In order to synthesized nanoparticles and nanocomposite of the desired size, shape, stability, and high quality, optimization is crucial. To achieve the best results, one parameter was changed at a time while keeping the others constant. This approach was based on prior research that identified several factors as the ideal conditions for nanoparticle creation. As a result, the effects of pH, temperature, amount of phytolacca dodecandra leaf extract, metal salt concentration, and plant to precursor volume ratio were all optimized [27].

3.7 Green synthesis of the CuO, ZnO NPs, and CuO/ZnO NCs

Using the aqueous extract of *phytolacca dodecandra* leaf, CuO NPs, ZnO NPs, and CuO/ZnO nanocomposite were synthesized using a method that had been previously described with some improvements [18].

3.7.1 Green Synthesis of CuO nanoparticles

A combination of metal solution with a plant extract can generates nanoparticles by reducing the metal ions. The active chemicals in the plant extract are responsible for reducing copper ions to create stable copper nanoparticles [59]. Accordingly, the CuO

NP was synthesized in this study using a green approach that involved using *phytolacca dodecandra* leaf and 0.1 M pentahydrated copper sulphate. In brief, the leaf extract and 0.1 M pentahydrated copper sulphate were mixed in a 1:1 v/v volume ratio. Then, 1M NaOH was added to the mixture and stirred continuously until the pH of the mixture reached 10. The solution was swirled at 70°C for 90 min. Until the blue solution turned green and a dark brown precipitate appeared. The appearance of the dark brown precipitate indicated the reduction of all copper ions and the formation of CuO NPs. The precipitate was separated, by using centrifuged for 15 min at 12,000 rpm. The precipitate was then cleaned several times with ethanol and distilled water to remove any contaminants. After that, the precipitates of the synthesized copper nanoparticles were collected using a crucible and allowed to dry at room temperature. The produced copper nanoparticles were then tested for thermal stability and calcined for approximately two hours at 400°C in a preheated muffle furnace. The resulting fine, black CuO nanoparticles were sealed in an airtight container [92, 93].

3.7.2 Green Synthesis of ZnO Nanoparticles

ZnO NPs were successfully synthesized using *phytolacca dodecandra* extracts and 0.1M zinc sulphate heptahydrate mixture in a 1:1 volume ratio. The mixture solution was adjusted pH of 9 using 1 M NaOH under stirring prepared. After that, the solution was mixed with 70 °C and 90 min continuously, and a white precipitate was observed in the solution. We collected precipitating items and centrifuged for 10 min at 4000 rpm. Finally, the resulting precipitate was washed several times with distilled water and ethanol, the precipitate was collected, dried at room temperature. The resulting solid was then calcined at 450 °C for 2 hour [94].

3.7.3 Synthesis of composite CuO/ZnO NPs

Phytolacca dodecandra leaf extract has been used to successfully synthesized CuO/ZnO NCS in an environmentally acceptable manner. In brief *phytolacca dodecandra* leaf extract, 0.1M zinc sulphate heptahydrate, and 0.1M copper sulphate pentahydrate were mixed in a 1:1:1 and 1:2:1 v/v in an enlimenary flask and then the pH of the mixture was adjusted to 10 by adding an aqueous solution of NaOH (1 M) drop-wise. After that, the mixed solution was heated by 70°C for 90min resulting white precipitate color was observed. The resulting precipitate was then centrifuged

for 10 minutes at 4000 rpm, and the precipitate was collected, dried at room temperature, calcinated at 450 °C for 2hr using muffle furnace [15].

3.8 Characterization of CuO, ZnO NPs, and Composite CuO/ZnO NCs

The synthesized nanoparticles have been characterized using FTIR, UV- Vis and XRD spectroscopy techniques. Thus, the functional groups of bioactive chemicals that were employed to bio reduce metal ions, *phytolacca dodecandra* leaf extract and the synthesized (calcinated or uncalcinate) CuO, ZnO NPs, and CuO/ZnO composite were identified using FT-IR spectroscopy. Initially, a drop of *phytolacca dodecandra* extract was combined with KBr powder to create a paste. The paste was then put into the FT-IR and scanned in a wave number range of 400 to 4,500 cm^{-1} at a resolution of 8 nm [87].

The absorption spectrum and band gap energies of the synthesized NPs were measured/calculated using UV-visible spectrophotometer in the wavelength region of 800 to 200 nm and distilled water was used as blank (reference) solution [95].The crystalline size of the synthesized CuO, ZnO NPs, and ZnO/CuO NCs were obtained by X-ray diffractometer which was record in the range between the 2theta angles 10^o and 80^o using Cu Kα (=1.54 Å) radiation operated at 40kV and 30 mA [96].

3.9 Anti-bacterial Activity of the synthesized CuO, ZnO NPs and CuO/ZnO NCs

The antibacterial activity of synthesize NPs, NCs and plant leaf extract were investigated for gram negative bacteria (*Escherichia coli, Salmonella*) and gram positive bacteria (*Staphylococcus aureus)* by using agar well disc diffusion method. Common available antibiotics like *Gentamicin (*positive control) and distilled water (negative control) were utilized. All the bacterial strains were cultured on selective agar media (macckonkey agar, S.S agar and manitol salt agar). Thus, 50µl of Muller Hinton (MH) agar plates were prepared, sterilized and solidified each bacteria was spread on the media. Then 25, 50 mg/L concentrations of green synthesized calculated CuO, ZnO NPs, and CuO/ZnO NCs and leaf extract of *phytolacca dodecandra* were added on each bacterial spread media at equal distance, solidify and were kept for

incubation at 37 ℃ for 48 hr. After the incubation time end the zone of inhibition was measured with transparent ruler in Millimeter [87, 97].

3.10 Photo catalytic activity of synthesized NPs and Nanocomposite

3.10.1 Photo catalytic degradation of MB dye

Photo catalytic activity and degradability of CuO, ZnO NPs, and CuO/ZnO NCs were evaluated by monitoring the degradation of methylene blue (MB) under sunlight irradiation. The degradability performances of CuO, ZnO NPs and CuO/ZnO NCs were seen by optimizing four independent variables like, NP sand NCs concentration (10-60mg, between 10mg difference), initial concentration MB (10-36mg/L), pH (2-12 between 2 difference). A dye solution with CuO, ZnO NPs, and CuO/ZnO NCs were placed under the exposure of natural summer sunlight irradiation for different time intervals between (20-140) min at regular time intervals (every 20 min).After degradation of dye sample was withdraw and centrifuge at 6000 rpm for 10 min to separate NPs from the degraded dye solution and then the solution was subjected to UV-Vis spectrophotometric analysis in the range of 300 to 800 nm [98, 99]. Degradation percentage of dye solution was calculated from the following equation:

$$\text{Percent of degradation} = \frac{\text{Ao}-\text{At}}{\text{Ao}} \times 100 \quad \ldots\ldots\ldots\ldots\ldots\ldots\ldots\ldots \quad (1)$$

Where A_o is the initial absorbance of dye and A_t is the absorbance of dye at any time.

3.10.2 Reusability of adsorbent (CuO/ZnO NCs)

The synthesized CuO/ZnO NCs recyclability or reusability is crucial factors in the selection of practical and affordable photo catalysts when the solar light irradiation method is applied. The study examined the reusability performance of CuO/ZnO NCs through three cycles of MB photo degradation. The optimized parameters including (pH 10, adsorbent dose (10 ppm), adsorbate dose 40 mg, and contact time 120 min) were implemented for this purpose. The mixture of MB dye and NCs was exposed to sunlight irradiation for the optimal time. After completing a given time, the NPs and degraded MB dye solution was isolated by centrifugation at 4000 rpm. After separating the NCs, measure the absorbance by using UV-Vis spectrometer (200-800nm). Then it has been used again 2cycle for MB dye degradation test. Similar

procedure has been employed for subsequent reusability test. Finally, the degradation performance for each test were calculated using equation (1) [100, 101] .

CHAPTER FOUR

4. Results and Discussion

4.1 Phytochemical Analysis of the Plant Extracts

The confirmatory qualitative test, which involved color changes, indicated the presence or absence of beneficial bioactive ingredients such as alkaloids, tannins, flavonoids, terpenoids, saponins, and phenolic active compounds in *phytolacca dodecandra* leaf extracts [102].

The result the presence of alkaloids, tannins, saponins, flavonoid, terpenoids and polyphenols containing O-H, N-H and C=O, C-H, C-C, -OH phenolic and other stretching bonds at various level. Thus, flavonoids and saponins were found in moderate level, whereas alkaloids, polyphenols, terpenoids and tennis were found in highest level. The details of the result are shown in **Figure 5 and Table 2** As a result *phytolacca dodecandra* leaf extract is composed of phytochemicals which are capable of reducing the Cu^{2+}, Zn^{2+} ion by donating electrons, capping and stabilizing the formed nanoparticles.

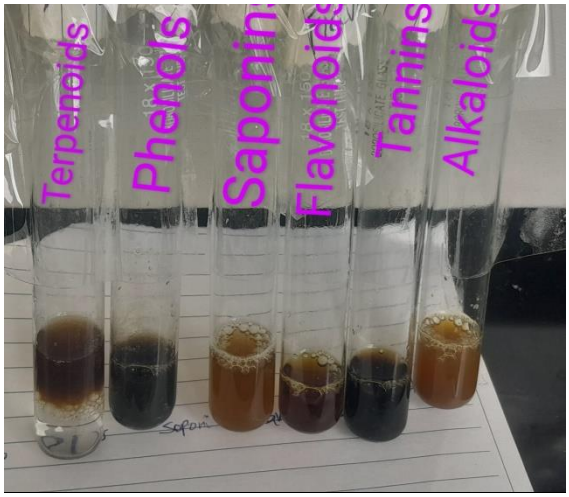

Figure 5. The color change observed when the leaf extract of *phytolacca dodecandra* was tested for the presence of bioactive components (phytochemicals).

Table 2. The phytochemical screening of the *phytolacca dodecandra* leaf

No.	Metabolites(bio actives)	Observation	***Phytolacca dodecandra*** aqueous leaf extract
1	Alkaloids	Yellow precipitate color	++
2	Tannins	Brownish green color	++
3	Phenols	Bluish black color	++
4	Saponins	Foam formation	+
5	Flavonoids	Brownish precipitate color	+
6	Terpenoids	Formation of layer and reddish brown color	++

Note: ++ ***Sign indicate the most presence of bioactive component and,*** + ***Sign indicate the more present of bioactive component.***

4.2 Optimization of Parameters for the Synthesis of CuO, ZnO NPs, and CuO/ZnO NCs

The optimization different parameters by using Uv-visible spectrophotometer the optimized parameter selected based on those points (1). Sharpness and intensity of the absorption peak was increased (2).The yield of NPs and NCs and the absorption peak shifts to blue shift. Those pointes indicate desired size, shape, stability, and high quality NPs and NCs were synthesized [103, 104].

4.2.1 Optimization of Precursor Metal Salt Concentrations

To achieve an optimum condition for the synthesis of nanoparticles, the amount of the plant extract with the concentration of metal precursors used should have matched [105]. The result of the present study is given in **Table 7** and **Figure 18 (at appendix)**, that as the concentration of the solution metal precursor was increased the sharpness and intensity of the absorption peak were increased. However, when the metal precursor concentration was further increased, the intensity of the absorption peak decreased.

Consequently, it was shown that raising the concentration of metal precursor beyond the optimal value led to a drop in the yield during the nanoparticle production process. This is probably because, instead of causing capped nanoparticles and nanocomposite to develop in a colloidal solution, the greater concentrations of $CuSO_4.5H_2O$ and $ZnSO_4.7H_2O$ serve to promote the agglomeration of the CuO and ZnO particles [106]. It was determined that the ideal concentration for the synthesis of ZnO, CuO NPs, and CuO/ZnO NCs was 0.1 M.

4.2.2 Optimization of *phytolacca dodecandra* leaf extracts Concentration

The process of synthesis of NPs using plant extracts relies on the specific phytochemicals found in plant extracts and the amount used. The amount of plant extracts used in the preparation of nanoparticles influences how long it takes to synthesize them. A previous report found that using more extracts can speed up the synthesis process of nanoparticles. This is because there are more chemical ingredients (phytochemicals) available in the solution that bind with the precursor to synthesize nanoparticles rapidly and stabilize them [107].

The result was noticed that the absorption and peak prominence got better when the amount of *phytolacca dodecandra* powder increased from 3% to 7%w/v. Then 4% was optimized because a sharp peak with high intensity was obtained. The result is depicted in **Table 7** and **Figure 19 (at appendix)**. The absorption spectrum narrows with increasing intensity when the amount of *phytolacca dodecandra* leaf powder increases, indicating that the nanoparticle size is more uniform and stable. However, at low concentrations of *phytolacca dodecandra* leaf powder, it may not be possible to completely reduce the 0.1 M copper and zinc precursor.

This is demonstrated by the increase in absorbance values with the increase in *phytolacca dodecandra* leaf extract, which shows higher production of NPs. The broad absorption spectrum intensity increases and absorbance values fall after reducing from a larger amount of 7% to a lower amount of 2% of *phytolacca dodecandra*, indicating that there was less control over the particle size [108].

4.2.3 Optimization of volume ratio of precursor and plant

The phytochemicals present in the plant extract react with the reagent to form nanoparticles with different purity [109]. If they are increased, they start reacting with each other and decrease the formation of nanoparticles. Among the tested ratio (1:1v/v) were found to be an optimal ratio as shown in **Table 7** and **Figure 20 (at appendix)**.

4.2.4 Optimization of pH

CuO, ZnO NPs and composite CuO/ZnO NPs size and texture were impacted by the solution's fluctuating pH levels. Furthermore, the size and form of the produced nanoparticles have been manipulated by adjusting pH levels [109]. Hence, the solution's pH ranged from 7 to 12 was tested in this study, and the results are given in **Table 7** and **Figure 21 (at appendix)**. The absorption peak of NPs increased with increasing solution pH. The maximum absorption peak intensity was observed at pH 9 and 10 for CuO/ZnO NCs, CuO and ZnO respectively. Thus, an optimum pH for the synthesis of CuO/ZnO, CuO and ZnO NPs was found to be 9 and 10 respectively.

4.2.5 Optimization of the Ratio of Precursors for Nanocomposite

To obtain the optimum ratio of CuO/ZnO NCs, different amounts of the metal precursor solution were used. The synthesis of the NCs was employed using different volume ratios of 1:1:1, 1:2:1 and 2:1:1 v/v of 0.1 M $ZnSO_4.7H_2O$, $CuSO_4.5H_2O$, and *phytolacca dodecandra* leaf extract. 1:1:1 and 1:2:1v/v was optimized because the absorption peak with high intensity was obtained at these ratios **Table 7(at appendix)**.

4.2.6 Optimization of Reaction Time

Reaction time is the time required for the completion of the reaction. Mainly, a plant extracted solution is mixed with the desired concentration of metal precursor and then heated under optimal conditions until the color of the mixture changes. NPs can undergo aggregation, shrink, or grow during long-term storage, and they also have a shelf life that eventually affects their overall potential [110].

The UV-Vis spectra of CuO, ZnO NPs, and CuO/ZnO NCs showed that 90 min sharp and intense peak show **Table 7** and **Figure 22 (at appendix)**. In general, controlling

all parameters, including temperature, pH, precursor, plant extract, and reaction time, should be highly considered to form specific NPs for the desired application.

However, controlling the constancy and aggregation of nanoparticles, adjusting crystal growth, morphology, size, size distribution, and separation of formed nanoparticles for more applications are the most challenging and problematic procedures and still in the development stage.

4.2.7 Optimization of Temperature

One significant element that influences the formation of metal oxide nanoparticles is temperature. A temperature range of 25°C to 100°C is recommended for the production of metal oxide nanoparticles [111]. Optimization was carried out at five different temperatures as show at **Table 7(at appendix)**. This allowed for the determination of the optimal temperature for synthesis of ZnO NPs, CuO/ZnO NCs and CuO which were optimized at 70°C. The findings showed that when temperature rose, so did the intensity of the NP and NC absorbance peaks.

This result may be owing to the fact that at higher temperatures, the reduction of metal ions to their nanoparticles is quick. However, when further increased in temperature beyond the optimized value, the absorption peak became less intense. This observation may also be due to the agglomeration of the NPs and NCs, possibly because the heat destroyed the reducing agents and capping agents found in the plant extracts [112].

4.3 CuO, ZnO and CuO/ZnO NPs

The green method was applied to synthesize CuO, ZnO NPs, and CuO/ZnO NCs using *phytolacca dodecandra* extract. The phytochemicals found in the extract acted as reducing agents to reduce the metal ions to their corresponding nanoparticles. When the *phytolacca dodecandra* extract was added to blue copper sulphate, at pH of 10, greenish color was formed; after 1:5hr of heating dark brown solid (precipitate) formed indicating the formation of CuO nanoparticles. When the *phytolacca dodecandra* extract was added, at pH of 9 to colorless zinc sulphate, a white precipitate was formed indicating the formation of ZnO nanoparticles. When the *phytolacca dodecandra* extract was added to the mixed solution of blue copper sulphate and zinc sulphate, at pH of 10 a light greenish blue precipitate was formed

indicating the formation of CuO/ZnO NCs. The mixture of the solutions obtained during the study is given in **Figure 6.**

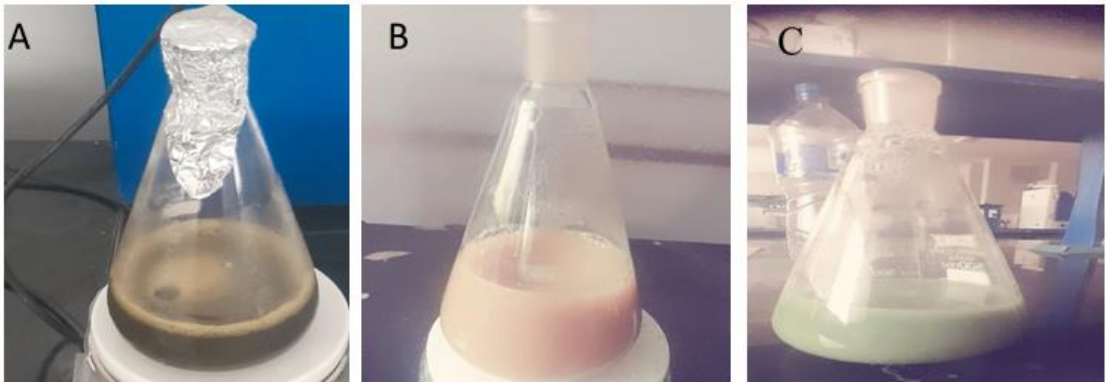

Figure 6. Synthesized nanoparticles and nanocomposite (A) CuO (B) ZnO (C) CuO/ZnO composite

4.4 Characterization of CuO, ZnO NPs and CuO/ZnO NCs

The final ZnO, CuO NPs and CuO/ZnO NCs formed were characterized using variety techniques including ,UV-visible spectrophotometer, FTIR and XRD [20].

4.4.1 Fourier Transform Infrared (FT-IR) Spectroscopy Analysis

FT-IR is used to identify phytochemicals that are involved in stabilizing, reducing, and capping. The various functional groups of the molecules present in the nanoparticles, and nano composite of *phytolacca dodecandra* are identified by FT-IR wavelength of 4000-400 cm-^{1}peaks [113].

Figure 7a the broad peak around 3460 shows the presence of phenol (-OH) compounds, due to hydrogen bond, which is possibly responsible for the stabilization process of the nanoparticles. The carbonyl groups appeared to confirm that compounds such as ketones, esters, and aldehydes are present [114]. The major and strongest vibrational modes FT-IR spectrum of Uncalcinate CuO NPs uncalcinate, ZnO NPs uncalcinate, 1:1:1 CuO/ZnO and 1:2:1 CuO/ZnO stabilized in *phytolacca dodecandra* leaf is those located shows **Table 3** and **Figure 7a**. This agrees with the conclusion that leaf extract of *phytolacca dodecandra* is composed of polyphenols, flavonoids, alkaloids and other similar phytochemicals containing O-H, N-H, -OH phenolic and C=O and other stretching bonds, which was confirmed by using FT-IR

spectra. **Figure 7b** displayed the FT-IR spectra of the green synthesized NPs and NCs where showed great changes relative to the uncalcinate NPs and CuO/ZnO NCs peaks and their intensities where observed. This indicated that the major biomolecules from the *phytolacca dodecandra* extract were removed to the surface of CuO, ZnO, and CuO/ZnO NCs. This mean no absorption peaks were found in different zones.

The successful synthesis of CuO and ZnO in all the samples was confirmed by the appearance of peaks at low wavelengths from 700 to 400 cm^{-1}. The spectra of ZnO, CuO,1:1:1(ZnO/CuO)NCs, and (1:2:1)ZnO/CuO NCs samples exhibited a peak in wavenumber of 412 cm^{-1}, 442 cm^{-1}, 437 cm^{-1}, and 426 cm^{-1} stretching vibration respectively [115].

Table 3. Fourier transforms infrared spectra absorption band (cm^{-1}) for *phytolacca dodecandra* leaf extract, uncalcinate ZnO NPs, CuO NPs, CuO/ZnO (1:2:1) NCs and CuO/ZnO (1:1:1) NCs.

Note; ***Absorption (AB)***

AB of leaf extract	AB of uncalcinate CuO NPs	AB of uncalcinate ZnO NPs	AB of uncalcinate 1:1:1CuO/ ZnO	AB of uncalcinate1:2:1CuO/ZnO	Description for stretching/vibrations/ bending
3460 2921	3431 2929	3446 2921	3305 2921	3416 2929	O-H in alcohol, phenol, C-H stretching. O–H stretch, -OH phenolic, 3500–2700 cm^{-1}
1810	1831	1860	1838	1824	Combination band for aromatic ring
1609	1617	1602	1602	1616	1600–1585 (m) carbonyl starching, C–C stretch (in–ring)aromatics starching
1384	1384	1293	1280	1378	C-O starching
964	957	957	950	964	910–665 N–H 1˚, 2˚ amines 900–675, (s)C–H aromatics
446	442	446,425	435	442	vibration/stretching Zn-O, and Cu-O NPs, since in all samples the absorption at this wave length was detected, Zn-O, Cu-O and Zn-Cu stretching

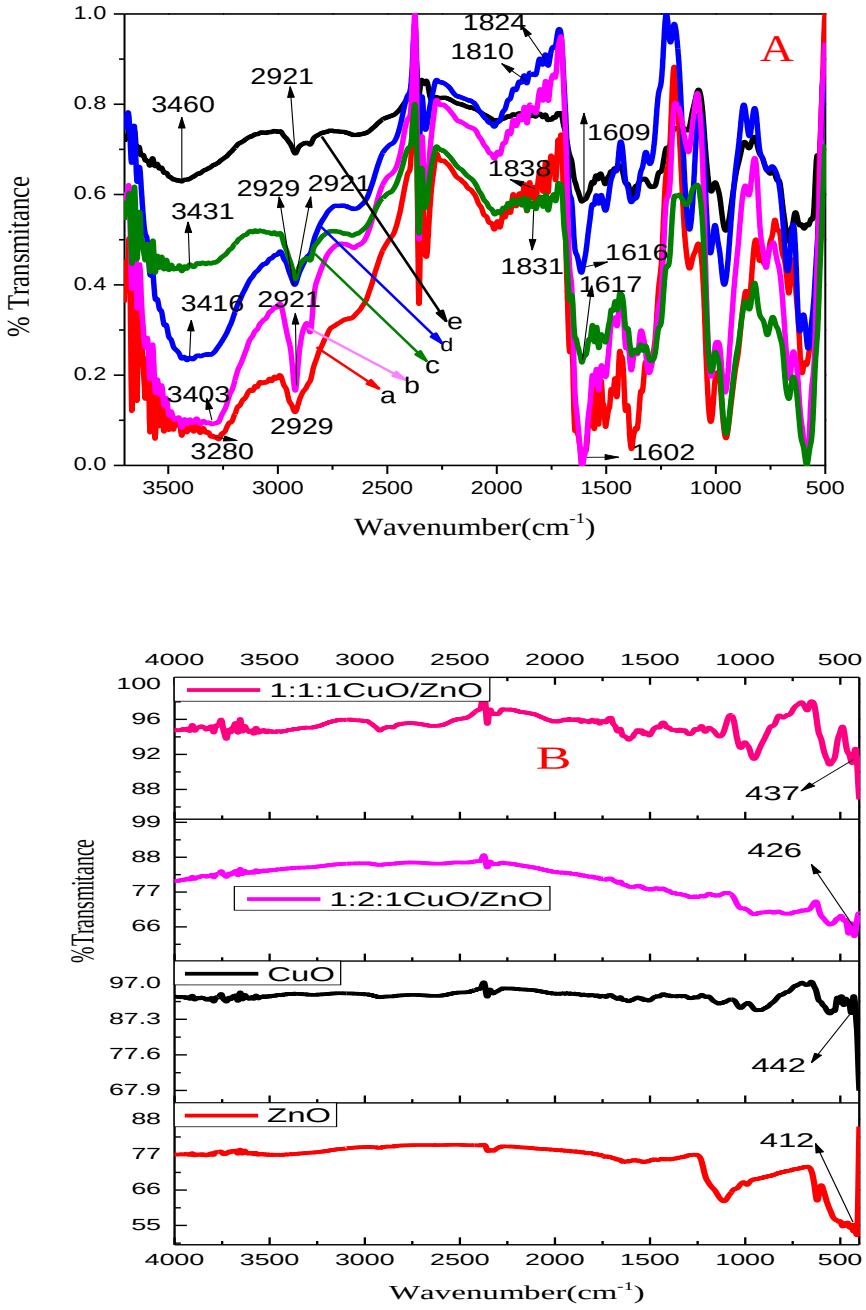

Figure 7. Fourier transforms infrared spectroscopy spectra of (A). **a**. uncalcinate 1:1:1CuO/ZnO **b**. uncalcinate ZnO **c.** uncalcinate CuO **d**. uncalcinate CuO/ZnO **e.** *Phytolacca dodecandra* leaf and (B). Calcinated NPs& NCs

4.4.2. X-Ray Diffraction (XRD) Analysis

The crystalline structure and degree of phase purity of the synthesized ZnO NPs, CuO NPs, and ZnO/ZnO NCs were characterized by XRD [116]. The greenly synthesized ZnO, CuO NPs and 1:1:1, 1:2:1 CuO/ZnO NCs by employing the leaf extract of

phytolacca dodecandera were further demonstrated and confirmed by the characteristics peaks observed in the XRD spectra, **Figure 8**.

Using corresponding miller indexes of 31.8796^{o} (100), 43.5229^{o} (002), 36.4627^{o} (101), 47.6627^{o} (102), 48.890^{o} (012), 56.7765^{o} (110), 63.0719^{o} (103), 66.4675^{o} (200), 68.160^{o} (112), 69.2026^{o} (201), and 72.5333^{o} (004), all peaks in the XRD patterns of the ZnO are consistent with the JCPDS (**card no. 00-036-1451**). Correspondingly, the diffraction peaks of CuO NPs was 32.6013^{o} (110), 35.5843◦ (11-1), 35.7490◦ (002), 38.9150◦ (111), 39.0797◦ (200), 46.4366◦ (112), 48.8889◦ (202), 53.7935^{o} (020), 56.7765^{o} (021), 58.3503^{o} (202), 61.8458^{o} (113), 65.8719^{o} (022), 66.4026^{o} (200), 72.6980^{o} (31-1) and 75.3333^{o} (220). All peaks in the XRD patterns of the CuO are consistent with the JCPDS (**card no. 00–048–1548**) data of the copper oxide. According to the XRD patterns of the two samples (ZnO-CuO NCs and ZnO, CuO NPs), neither a secondary phase nor any discernible impurities are present in the samples [117].

The synthesized of CuO/ZnO NCs are compared to the acquired diffraction peaks of both CuO and ZnO NPs the intensity of the peaks increases, indicating good crystallinity and purity. Moreover, the intensities of the peaks linked to CuO in the CuO/ZnO diffraction pattern appeared to be higher than those of ZnO NPs. The most intense peak in the (1:2:1) CuO/ZnO XRD result (002) 35.570 and (111) 38.900 indicates that the majority of the crystals are dominated and were identified at 2θ for ZnO nano composites with varying CuO concentrations. Because of the increase in inter planar spacing, variations in the effective ionic radius of atoms significantly affect peak positions and lattice characteristics, as shown in **Figure 8**. This point to a higher fraction of zinc–copper NPs bimetallic structure and strong crystallinity.

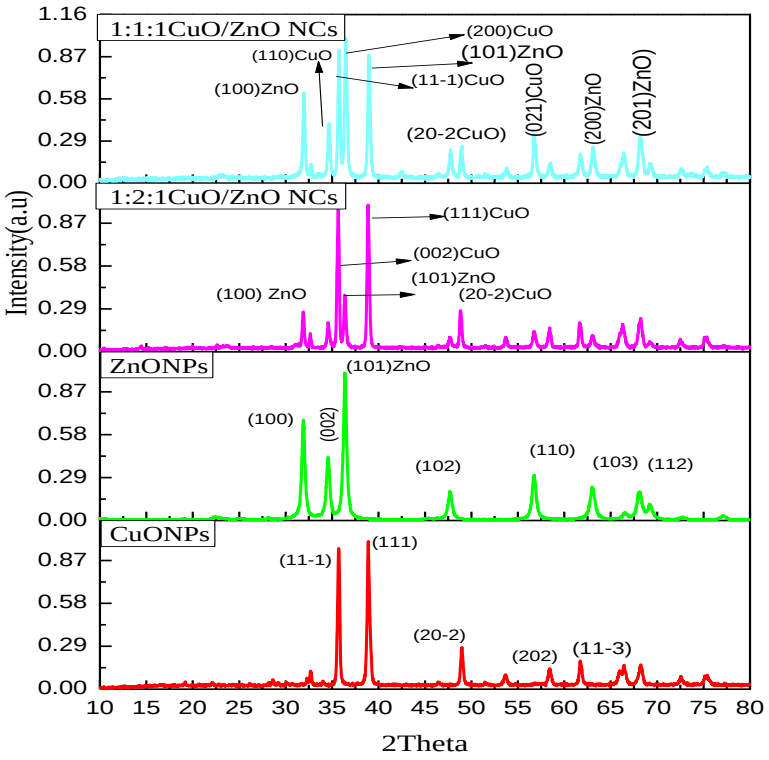

Figure 8. XRD spectra of ZnO, CuO NPs, CuO-ZnO (1:2:1) and CuO-ZnO (1:1:1) composite.

Using the Debye Scherer formula, the typical crystallite size of ZnO, CuO NPs, and associated CuO/ZnO NCs was determined from a subset of main peaks (sharpest reflection).

$$D = \frac{0.9\lambda}{\beta cos\theta} \quad \text{.....(3)}$$

Where k represents the Scherer constant k = 0.90, λ = 0.15406 nm is the wavelength of the incident Cu Kα radiation; β represents the full-width at half-maximum (FWHM) of the respective peak [118].

Table 4. Evaluation of crystal size D from XRD results of ZnO.

ZnO NPs				
Peak Position2θ (°)	FWHM(Radians)	Miller Indices	D (nm)	D nm(average)
31.90518	0.5959	100	17.97794	17.09418
34.57094	0.49797	002	16.70794	
36.39043	0.48299	101	17.31387	
56.751	0.55133	110	16.37698	
CuO NPs				
35.70623	11-1	0.29072	28.7081	19.84306
38.91377	111	0.35925	23.4528	
48.97477	20-2	0.32836	26.5851	
65.66878	11-3	15.11414	0.625558	

Table 5. Evaluation of crystal size D from XRD results of 1:1:1 and 1:2:1CuO composite.

1:1:1CuO/ZnO NCs				
31.96754	100	0.27531	30.01623	27.88121
35.74603	11-1	0.28811	28.97202	
36.47626	101	0.3308	25.28563	
38.97684	200	0.30924	27.25096	
1:2:1CuO/ZnO NCs				
35.65151	002	0.26833	31.0994	30.23975
36.38441	101	0.29093	28.74328	
38.88761	111	0.28887	29.16456	
48.84692	20-2	0.27307	31.95172	

The average crystalline size of the CuO/ZnO rose as the ratio of CuO increased, according to the XRD examination. This could be as a result of the differences in copper and zinc ion sizes.

For ZnO NPs, CuO NPs 1:1:1 and 1:1:2:1 (CuO/ZnO) NCs, the corresponding particle sizes were 17.1, 19.8, 27.9, and 30.2 nm. This study confirms that there is an inverse relationship between size and band gap.

4.4.3 UV-Vis Analysis

UV–visible spectra could provide useful information about the electronic absorption properties, energy band gap of the samples and is one of the most widely used simple and sensitive techniques for the identification of the position, shape and intensity of the surface Plasmon resonance of nanoparticle formation [119].

The obtained CuO, ZnO NPs and, CuO/ZnO NCs displayed the characteristic surface plasmon resonance (SPR) band in the spectral range of 270-500 nm. The nanoparticle and nano composite CuO NPs at 401nm, ZnO NPs at 375nm, 1:1:1CuO/ZnO NCs at 411nm and 1:2:1 CuO/ZnO at 418nm NCs absorption peaks were observed **Figure 9**. This is in agreement with the earlier studies on the green synthesis [120].

The combination of CuO with ZnO red shifted the maximum absorption wavelength due to increased surface defects and oxygen vacancies. [121].

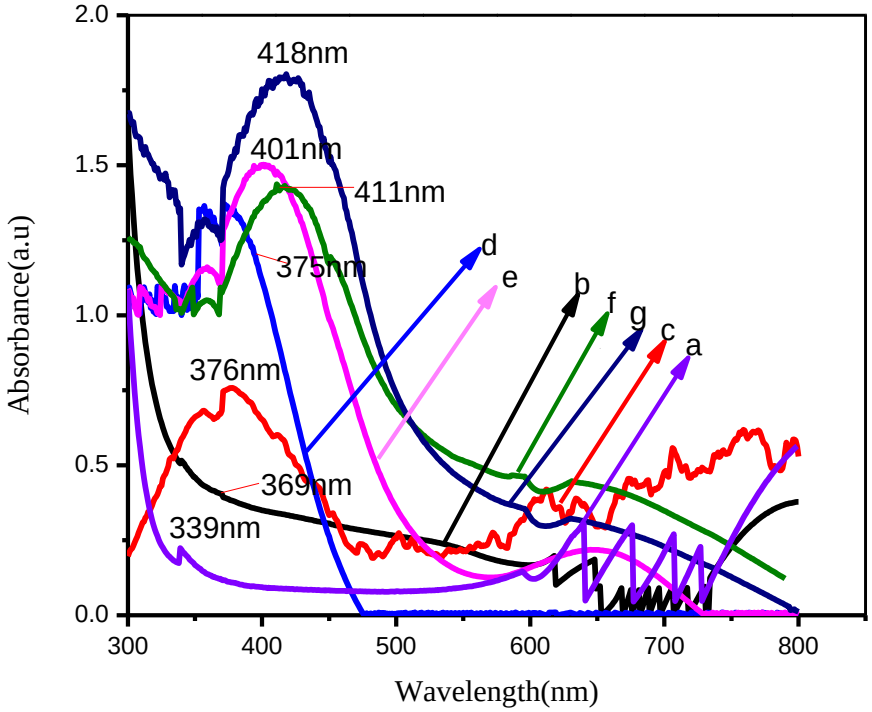

Figure 9. UV-Visible spectra of (a) $ZnSO_4.7H_2O$ (b) $CuSO_4 \cdot 5H_2O$ (c) Leaf extract of *phytolacca dodecandera* (d) ZnO (e) CuO NPs (f) (1:1:1) CuO/ZnO NCs (g) (1:2:1) CuO/ZnO NCs.

Band gap energy calculation

By using Tauc's plot and the following equation, the band gap energy values for the produced bare ZnO, CuO NPs and ZnO/CuO nano composites were determined from the UV-visible spectra.

$$(\alpha h\nu)^n = k(h\nu - Eg) \quad \text{..... (2)}$$

Where Eg is the band gap energy in eV, α is the absorbance value, ν is the frequency, h is Planck's constant, k is a constant, and n is equal to 1/2 and 2 for a direct and indirect transition, respectively.

The optical band gap energies of ZnO, CuO NPs, and the 1:1:1, 1:2:1 CuO/ZnO NCs were determined to be 2.83, 2.6, 2.4, and 2.3 eV, respectively, as shown in **Figure 10**. The red shift in the absorption spectra of the 1:1:1 and 1:2:1 composite is the cause of the decrease in band gap. The bulky band gaps of ZnO NPs (2.83 eV) and CuO NPs

(2.6 eV) are larger than the band gap of the produced 1:1:1 and 1:2:1 CuO/ZnO composite samples. Due to quantum confinement effects, the band gap energy of CuO NP was somewhat greater than the published value for bulk CuO (1.2 eV) [122]. These band gap values indicate the materials potential for use in photo catalysis when exposed to solar light.

The interaction between ZnO and CuO, which results in the creation of mixed composites, is confirmed by the noticeable fluctuation in band gap values. This means that the higher band gap energy was decreased by adding lower band gap energy to the higher band gap energy. Consequently, compared to ZnO alone, the ZnO/CuO NCs photo catalytic activity increased [123].

The photo catalytic performance of a photo catalyst greatly depends on its band-gap energy. For an efficient photo catalyst, the band gap energy should be fewer than 3 eV to extend the light absorption into the visible range to optimally utilize the solar energy. This indicates that the photo catalytic activity of the nanoparticles increases with narrower band gaps [124]. For this reason, in this work, 1:2:1 and 1:1:1 CuO/ZnO NCs show stronger photo catalytic activity than ZnO and CuO NPs.

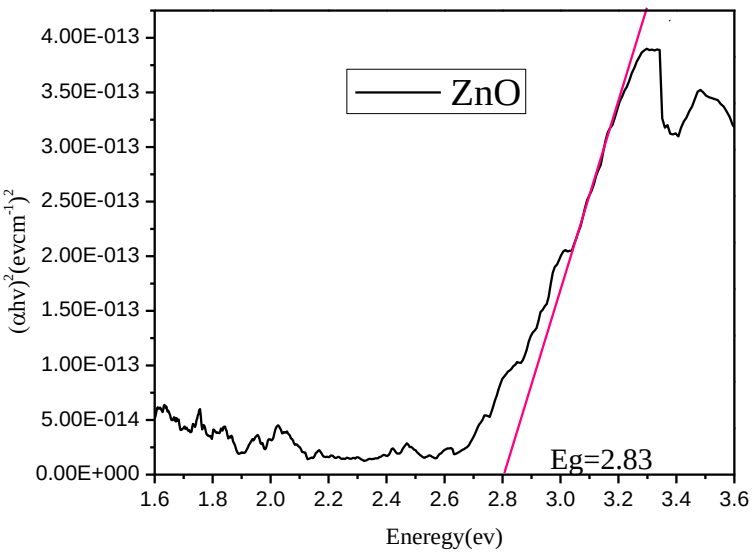

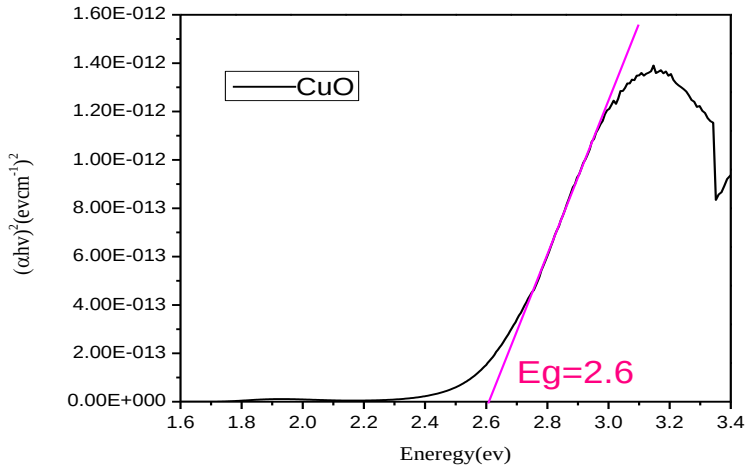

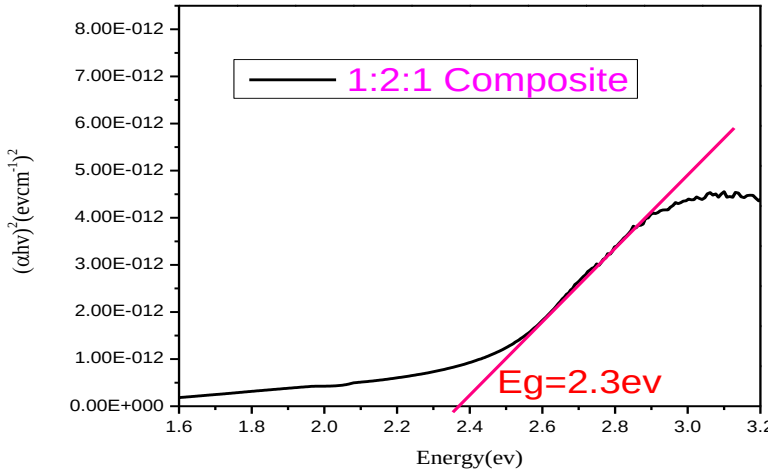

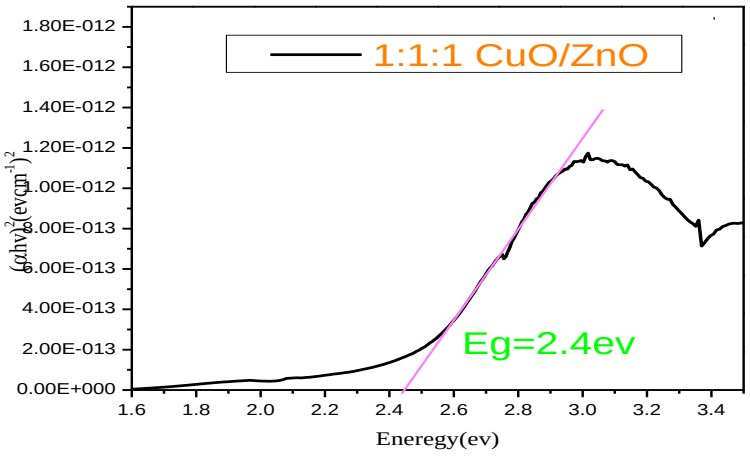

Figure 10. Tauc's plot for optical band gap energy of ZnO NPs, CuO NPs, 1:2:1 CuO/ZnO composite and 1:1:1 CuO/ZnO composite

4.5 Anti -bacterial Activity of CuO, ZnO NPs and CuO/ZnO NCs

The physicochemical features of nanomaterials, such as surface area, particle size, solubility, reactive oxygen species (ROS) production, and surface charges, all have a complex impact on their antibacterial activity. There are five antibacterial mechanisms of ZnO, CuO NPs and CuO/ZnO NCs have been proposed, which are (1) ROS generation through photocatalytic activity; (2) induction of oxidative stress; (3) attachment of the ZnO NPs to the bacteria cell walls; (4); release of Zn, Cu (II) ions; and (5) genotoxicity [125].

CuO, ZnO NPs, and CuO/ZnO NCs all kill bacteria by converting or adhering to the natural metalloproteinase components, as well as by releasing reactive oxygen species (ROS). CuO NPs, ZnO NPs, (1:1:1) CuO/ZnO, and (1:2:1) CuO/ZnO NCs were examined for their antibacterial properties utilizing varying concentrations of 25 mg/L and 50 mg/L. For both bacterial strains, CuO NPs and ZnO NPs showed less inhibition zones for both 25mg/L and 50mg/L doses as compared to the CuO/ZnO nano composite. 50mg/l of 1:2:1 CuO/ZnO NCs exhibited an inhibition zone on both gram-positive and gram-negative bacteria *(Staphylococcus aureus, Escherichia coli and Salmonella)* with maximum inhibition zones of 20.33±0.5, 15.66±0.7, and 19.66±0.5 mm depending on the positive control (gentamicin), **Table 6**. This is because of the combination of CuO and ZnO in the nano composite has a freer surface that can produce a higher amount of ROS compared to CuO and ZnO alone; adding CuO to ZnO produces more surface defects on CuO /ZnO.

When the surface has more defects, it also has more ROS; this causes more bacteria to be prevented from growing. When the energy band gap is smaller, the antibacterial activity increases because the electrons can move more easily from the valence band to the conduction band, and it can increase the radical compounds, effectively killing the bacteria [94, 126].

Figure 11 and **Table 6** indicate that as CuO, ZnO NPs and 1:1:1, 1:2:1CuO/ZnO NCs concentrations (25 mg/L) fall, the suppression of bacterial growth decreases for all samples. The antibacterial activity of all samples further improved with increased concentration [127]. Finally, this study indicated that Gram-negative bacterial strains were more sensitive in comparison to Gram-positive strains against the tested nano composites, and disclosed the potential application of the nano composites as

appropriate candidates for successful minimization of bacterial infections that may occur. Because Gram negative bacteria have thin peptidoglycan cell wall, which is easier to penetrate in G− bacteria.

Escherichia coli

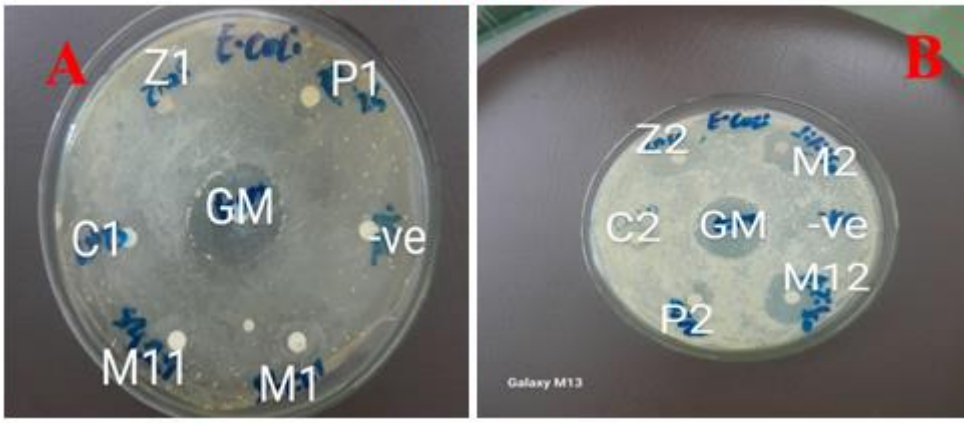

Salmonella

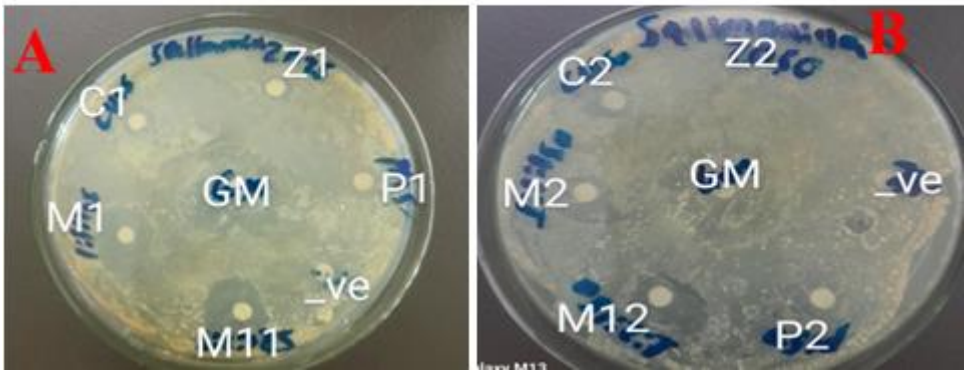

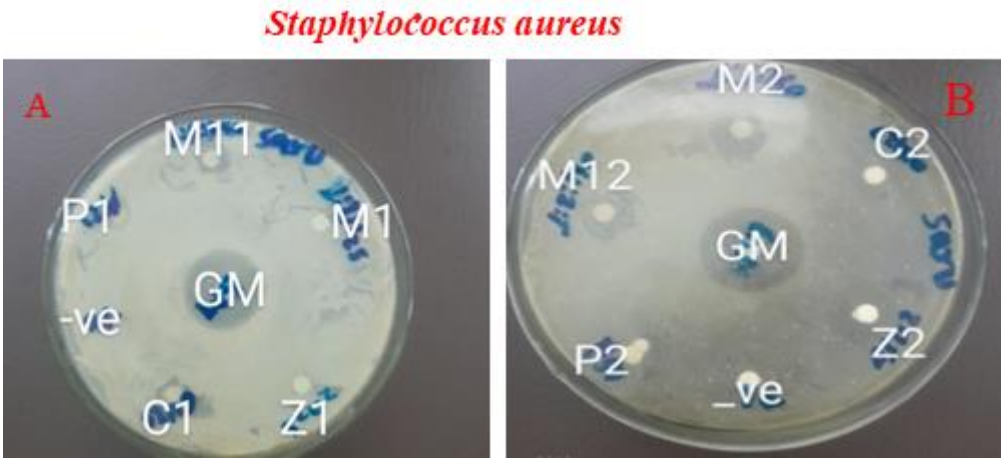

Note:

- ***M1=25mg/L of CuO/ZnO(1:1:1), P1=25mg/L of plant crude***
- ***M2=50mg/L of CuO/ZnO(1:1:1, P2=50mg/L of plant crude***
- ***M11=25mg/L of CuO/ZnO(1:2:1), Z1=25mg/L of ZnO NPs***
- ***M12=50mg/L of CuO/ZnO(1:2:1), Z2=50mg/L of ZnO NPs***
- ***C1=25mg/L of CuO NPs, -ve=negative control(Distilled water)***
- ***C2=50mg/L of CuO NPs, GM=gentamicin(positive control)***

Figure 11. Diagram of Zone of inhibition for microbial activities of plant crude, NPs and NCs with in different concentration (A) represents 25mg/L and (B) represent 50mg/L

Table 6. Comparative antibacterial activity of green synthesized CuO NPs, ZnO NPs, 1:1:1 CuO/ZnO, and 1:2:1 CuO/ZnO NCs.

Zone of inhibition (mm) mean ± SD				
NPs & NCs	Concentration(mg/L)	*Staphylococcus aureus*	*Escherichia coli*	*Salmonella*
ZnO	50	13.33±0.5	17 ± 1	15±1
ZnO	25	8.66 ± 0.5	11 ± 1	12.33±0.5
CuO	50	9 ± 1	15 ± 1	14.66±0.5
CuO	25	7.66 ± 1.5	12.33 ± 0.5	11±1
1:1:1CuO/ZnO	50	13.33 ± 0.5	19 ±1	18.66±0.5
1:1:1CuO/ZnO	25	8.66 ± 1.5	16.66±0.5	17.33±0.5
1:2:1CuO/ZnO	50	15.66 ± 0.7	20.33±0.5	19.66±0.5
1:2:1CuO/ZnO	25	12.33 ± 0.5	16.33±0.5	18.33±0.5
Plant(50mg/L)	50	8.33 ±0.5	12.66±0.5	10.66±0.5
Plant(25mg/L)	25	6.66 ± 0.5	9.33±0.5	9.33±0.5
Positive control(Gentamicin)	50	19.33±0.5	22.33±0.5	20±1
Negative control(distilled water)		0±0	0±0	0±0

Because of their special qualities and modes of action, nano composites are becoming more and more viable treatments for illnesses that are resistant to drugs (MDR) [128]. The (1:2:1) CuO/ZnO composite significantly increase ROS production, which is crucial for damaging bacterial cells. The slow release of Cu^{2+} ions from the composite contributes to its sustained antibacterial effect, as these ions can disrupt bacterial cell functions [129].

This event clearly indicates that the synthesized (1:2:1)CuO/ZnO composite could solve serious problems of human health, and to overcome this problem, they can be

utilized as a substitute for antibiotic-resistant strains of bacteria, economically viable and less toxic with high yields easily synthesized nanoparticles by using renewable natural materials

4.6 Photocatalytic Activity of Synthesized CuO, ZnO NPs, and CuO/ZnO NCs

The photo catalytic efficiency of the synthesized nano composite was studied under visible light irradiation. The degraded amount of MB dye was measured by recording UV-visible absorption spectra at 664 nm [130]. As shown in **Figure 15,** the attributed absorption peak of MB dye at 664 nm is continuously declining with time due to the photo degradation of MB dye into non-hazardous products. In 120 minutes of visible light irradiation, the dye was about to be highly degraded at 66% (ZnO NPs), 69.3% (CuO NPs), 81.5% CuO/ZnO NC (1:2:1) and 78% CuO/ZnO (1:1:1) NCs.

From the results, it is attributed that nano composite performed better photo catalytic activity as compared to bare ZnO, CuO NPs and ZnO/ CuO NCs material with lower CuO content degraded dye less effectively. Further increase of CuO and at optimized CuO (1:2:1) CuO/ZnO relative to(1:1:1) CuO/ZnO content in nanocomposite increase the rate of charge transfer and reduced the recombination rate of electrons and holes that increase photo degradation efficacy.

The probable reason behind the enhanced photocatalytic activity of a (1:2:1) CuO/ZnO NCs is because, (1) it enhances the mass transfer and diffusivity of the dye molecules and oxygen species; (2) effective separation of the photo generated charge carriers and an increased charge carrier lifetime; (3) large content of oxygen vacancies or defects that act as trapping centers for the photo generated electrons. These oxygen vacancies can also promote the absorption of O_2 that is converted into superoxide radicals (O_2^-). Furthermore, under photo irradiation, the nano composite works as a p-n junction, which reduces the recombination rate and aids in the split-up of electron hole pairs, and consequently, active hydroxyl radicals get produced in higher quantities [131].

The band gap and induced activation of light toward the visible light region or the transfer of photo activated electrons using a photo-sensitizer for the absorbed light in the visible region increase the electron-hole separation and accelerate the transfer of interfacial energy, thus causing efficient degradation of the dye and photo-

electrochemical activity toward water splitting. Overall, the above-mentioned results illustrate a better degradation efficiency of a CuO/ZnO NCs than its individual CuO and ZnO NPs components [132].

4.7 Factors affecting Photocatalytic activity of synthesized NPs, and NCs

4.7.1 Effect of pH

The impact of solution pH on dye degradation is well reported in the literature that the pH of the environment influences the surface charge of the photo catalysts [133]. Experiments were conducted with a fixed dye concentration of 10 ppm and 20 mg of CuO, ZnO, and CuO/ZnO NCs and by varying pH levels from 2 to 12.

The CuO, ZnO NPs and (1:1:1), (1:2:1) CuO/ZnO NCs surfaces acquire a negative charge in an alkaline pH, which promotes the emergence of reactive species that efficiently break down the cationic dye**.** There were no significant electrostatic interactions between these NPs and NCs surfaces and the MB dye molecules at acidic pH. Consequently, at acidic pH values, the degree of photo catalytic degradation of MB dye was reduced. The data clearly show that photo catalytic degradation is accelerated at pH values between 2-10, and that photo catalytic degradation efficiency of NPs and NCs decreases at pH 12. The generation of surplus anions is the rationale given [134].

Anions compete with dye molecules to adsorb on CuO, ZnO NP and CuO/ZnO NCs surface active sites, hindering adsorption and reducing photo catalytic degradation of MB dye. In basic pH, the dye degradation was higher, which is due to the negative charge on the surface of CuO, ZnO and CuO/ZnO NCs surface that enhances the reactive species formation [135]. The cationic dye was effectively attracted to the NP and NCs surface, enhancing dye removal through the oxidative process, particularly in basic media. Then the degradation efficiency of CuO, ZnO, (1:1:1) CuO/ZnO, and (1:2:1) CuO/ZnO were shown **Figure 12** and **Table 8 (at appendix)** where the optimal value were found as pH 9 and pH 10.

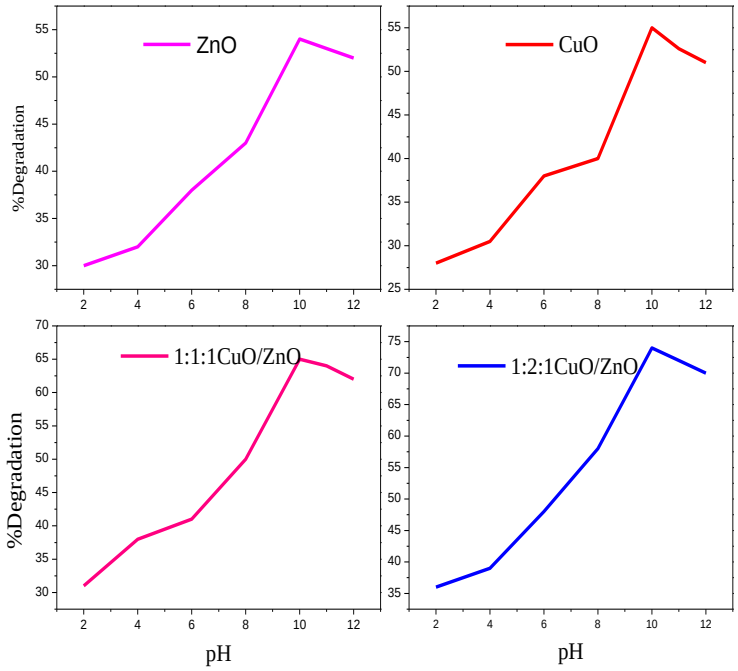

Figure 12. Effect of pH on the degradation of MB with in NPs and NCs catalyst

4.7.2. Dosage effect of the synthesized NPs and NCs on the Degradation of Dye

Dye degradation is significantly influenced by the dosage of NPs and NCs. By adding more catalyst, the dye was more readily broken down by photo catalysis [136]. Relative to a fixed dye concentration of 10 ppm and pH of 10, the degradation efficiency of MB shown in **Figure 13** and **Table 8 (at appendix)** where the concentration of ZnO, CuO, and (1:1:1)CuO/ZnO and (1:2:1)CuO/ZnO increased from 10 mg to 60 mg. This process is caused by the catalyst's increased active sites, which enable optimal dye molecule adsorption onto the catalyst's surface and the production of more reactive species for dye degradation [137].

However, a further increase in the catalyst loading after the optimum resulted in a decrease in the decolonization rate. The reason generally advanced for this result is that an increase in catalyst loading increases the active sites on the surface of the catalyst. However, as the number of nano catalysts increases, the transparency of the solution decreases. This phenomenon may be due to the hindrance and blocking of light penetration caused by the excessive amount of photo catalyst particles [138].

Therefore, the degradation rate tends to decrease as the catalyst dose increases above the optimum value. Then the degradation efficiency increase at the optimal value of 30mg and 40mg.

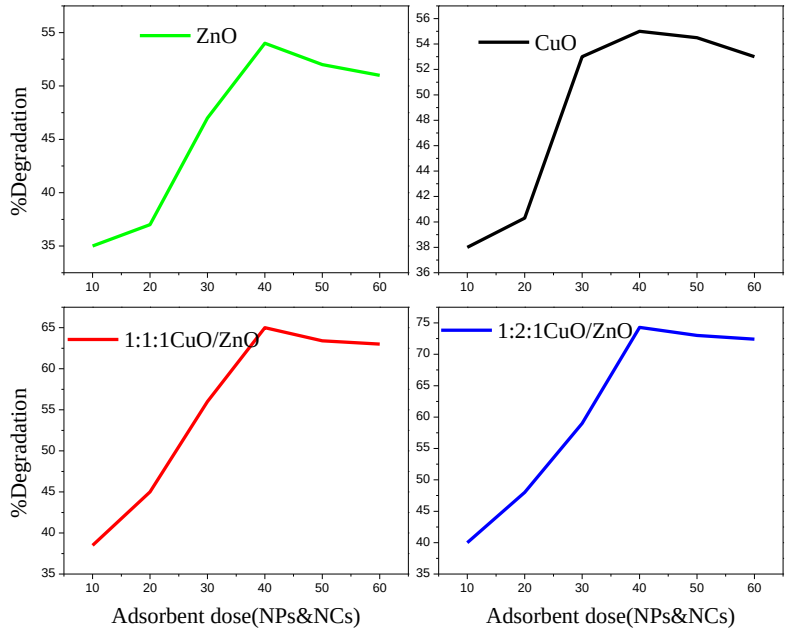

Figure 13. Effect of catalyst concentration (1:2:1 CuO/ZnO NCs, CuO NPs, ZnO NPs and 1:1:1CuO/ZnO NCs) on the degradation of MB

4.7.3 Effect of initial dye concentration

Investigating the impact of MB dye concentration on photocatalytic degradation at 10 to 36 ppm was done while maintaining consistent levels of nano catalysts (CuO, CuO/ZnO), pH, and irradiation period. The dye degradation decreased as the dye concentration increased as shown in **Figure 14** and **Table 8 (at appendix)**. This could be because of the higher concentration of dye obstructing the incident light's path, preventing light from reaching the catalyst surface and reducing degradation efficiency [139].

Furthermore, as a result of MB molecules adhering to the catalyst surface, fewer reactive species were produced, which in turn reduced the efficiency of degradation. Growing dye molecules may block active sites and lessen light's interaction with these sites, preventing the formation of hydroxyl radicals and superoxide ions (•OH/•O-) at the photo catalyst surface, which would accelerate deterioration. At high dye

concentrations, fewer hydroxyl radicals (•OH) and superoxide ions (•O-) are formed because a large amount of light can be absorbed by the dye molecules as opposed to the photo catalysts [140].

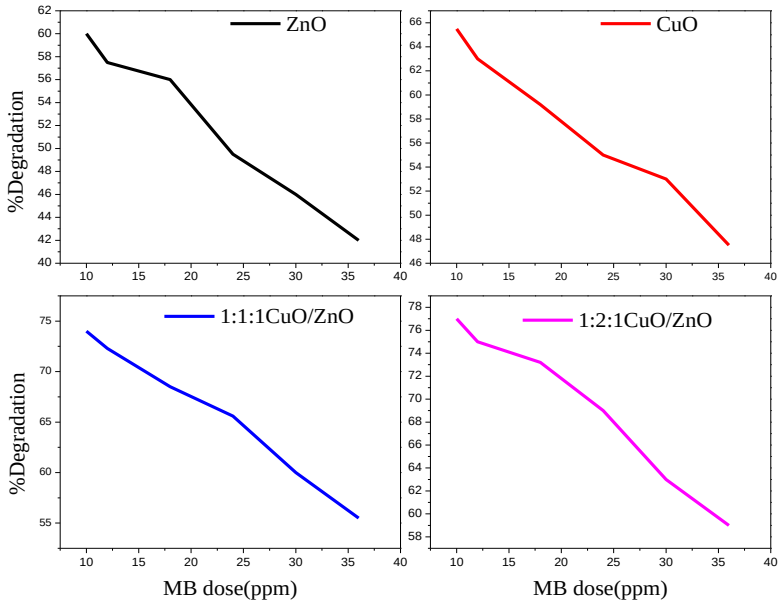

Figure 14.Effect of initial dye concentration on the degradation of MB with NPs & NCs catalyst

4.7.4 Effect of contact time

The degradation efficiency at various irradiation times (20–120 min) under ideal photo catalyst dosage, initial MB concentration and pH of solution were investigated as shown at **Table 8(at appendix)**. At 120 minutes, respectively, the maximum photo degradation of MB was reached for CuO NPs, ZnO NPs, 1:1:1CuO/ZnO NCs, and 1:2:1CuO/ZnO NCs photo catalysts. **Figure 15** illustrates how the degradation of MB progressed with increasing irradiation time. However, the degradation rate started to decline after 120 minutes.

It denotes the catalyst surface and dye particle repulsion, which slows down the rate of degradation. The photo catalytic degradation process slows down with time as degradation products vie with dye ions for adsorption on the catalyst surface. Reactive species (active site) subsequent breakdown and catalyst surface adsorption have a major impact on photo catalytic dye degradation [141].

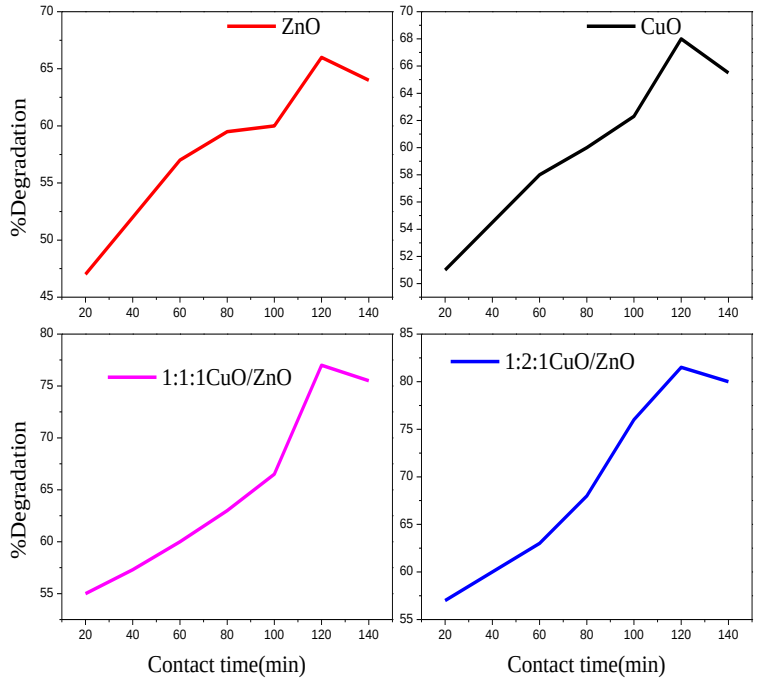

Figure 15. Effect of contact time on the degradation of MB with in NPs and NCs catalyst

The effectiveness of degradation of MB dye using *phytolacca dodecandra* leaf extract metal oxide composites as catalyst was investigated and the results are given at **Figure 15, and 23(at appendix).**

Hence, the maximum degradation capacity at optimized value of each parameters **(**contact time, catalysis dose, pH and adsorbant dose) were found to be 66%, 69.3% 81.5%, and 78% (ZnO NPs), (CuO NPs), CuO/ZnO (1:2:1) and CuO/ZnO (1:1:1) NCs, respectively. This result shows ZnO NPs have major short coming for photocatalytic activities like reduce effective optical absorption in UV region of the solar spectrum and easy recombination of photo generated electron-hole pair due to large band gap. In order to reduce these limitations metal ions combination or formation of hetero structures composed of CuO/ZnO NCs narrow band gap semiconductors were synthesized.

4.8 Mechanism of MB dye photo degradation

CuO valence band (VB) and conduction band (CB) are located above ZnO makes it thermodynamically advantageous for electrons and holes to move between the two.

For charge carrier transport, this makes ZnO and CuO green nano catalysts beneficial. As soon as a semiconductor absorbs visible light, an electron begins to excite from VB to CB, creating holes in VB. At the ZnO/CuO hetero junction interface, photo induced holes start to migrate in the opposite direction from the VB of ZnO to the CB of CuO since ZnO VB and CB are lower than CuO. Electrons start to move from the higher level CB of CuO to the lower level CB of ZnO [142].

This results in the accumulation of extra electrons in the CB of ZnO, which is used in the reduction of MB. By preventing electron-hole pairs from recombining to the same degree, this type of electron transfer increases the efficiency of photo degradation. When the electrons in ZnO CB were taken up by the molecular oxygen on its surface, superoxide radicals (O_2) were produced. The hydroxide ion, on the other hand, captured the photo induced holes in the VB by the production of active species, namely hydroxyl radicals. These free radicals react with MB to cause its full mineralization in CO_2 and H_2O [143, 144]. The possible mechanism is represented graphically in **Figure 16** with a description **a-e.**

a) Photocatalytic reactions are initiated when CuO/ZnO surface is exposed by a radiation of sun light (hv) equal to or greater than the CuO, ZnO and CuO/ZnO band gap
b) The photonic energy responds to excitation of the electrons and then produces electron-hole (e−/h+) pairs, one is a positively charged hole in the valence band (VB) and the other is a negatively charged electron in the conduction band (CB)
c) The electron-hole pairs can transfer to the CuO, ZnO and CuO/ZnO surface and be involved in redox reactions
d) The positive holes (H^+) created in the valence band reacts with absorbed water and hydroxide ions to produce powerful hydroxyl radicals. The hydroxyl radicals degrade the organic pollutants adsorbed on the surface of CuO, ZnO, and CuO/ZnO.
e) The conduction band electrons react with dissolved oxygen species to produce superoxide radical anions and then hydrogen peroxide.

Hydrogen peroxide will then react with superoxide radicals to form hydroxyl radicals which react with pollutants adsorbed on the surface of CuO/ZnO and then produce

intermediate compounds that converted to green compounds such as H_2O anCO_2 [145].

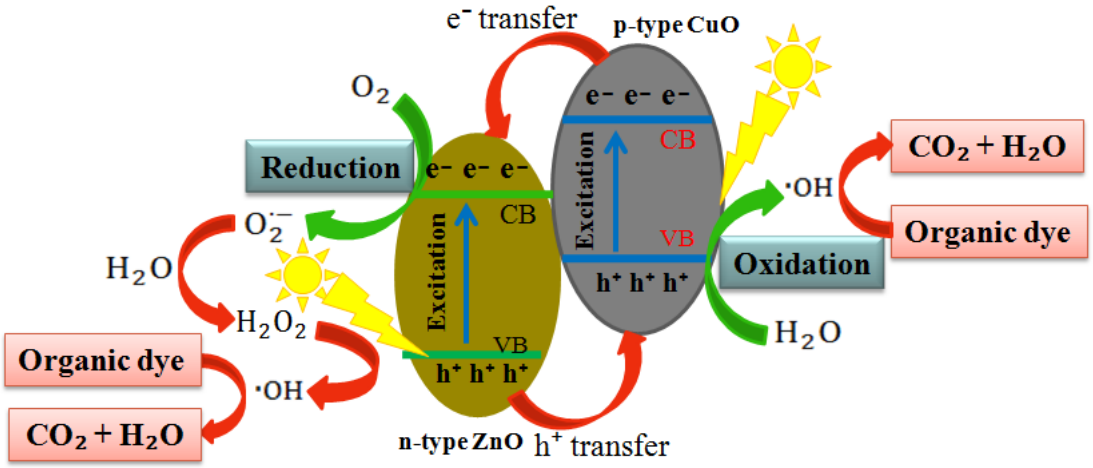

Figure 16. Mechanism of photo degradation of organic dye by ZnO/CuO hybrid nano composite.

4.9 Recyclability and Reusability of the catalysts

By lowering resource consumption, waste, and overall environmental effects, reusable catalysts in photo catalytic processes provide both environmental and financial sustainability. Reusability is a more sustainable option than single-use catalysts because the latter provide disposal issues, particularly when they contain hazardous or hard-to-recycle components. Stability of the catalyst is equally important for practical applications of photo catalysis as photo catalytic activity. In the catalytic test, the composite is utilized to examine its stability and recyclability over time [146].

Figure 17 shows that the CuO/ZnO (1:2:1) catalyst's stability, recyclability, and reuse were all confirmed. The result shows that, even after three rounds of identical conditions, the degradation of MB dye did not significantly reduce. The first cycle and third cycle of the CuO/ZnO (1:2:1) nano composites demonstrated approximately (82%) and (79.5%) photo catalytic degradation efficacy. The catalyst loss that occurs during sample utilization and the centrifugation procedure may be the cause of the little decrease in degradation efficacy. Therefore, it can be guaranteed that during the photo catalytic process, (1:2:1) CuO/ZnO nano composites show good stability and recyclability [147, 148].

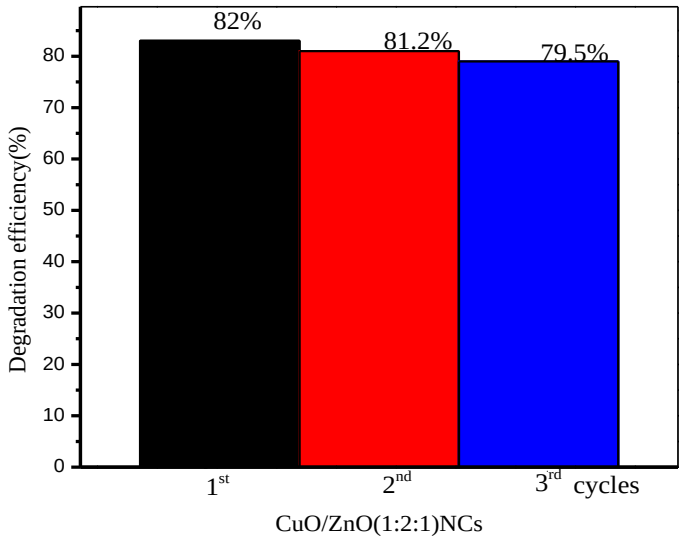

Figure 17. The degradation efficiency of (1:2:1) ZnO/CuO nano composites over continuous use in three cycles**.**

CHAPTER FIVE

5. Conclusion and Recommendation

5.1. Conclusion

Phytolacca dodecandra leaf extract was used as a capping and reducing agent instead of harsh, artificial reducing agents to synthesize CuO, ZnO NPs and CuO/ZnO NCs. Combining two semiconductors(CuO and ZnO), resulted in a more efficient active in MB dye degradation and antimicrobial activity than each material alone. Thus greenly synthesized CuO/ZnO with a ratio (1:1:1v/v), and (1:2:1v/v) CuO/ZnO have revealed stronger antibacterial activity than either of the CuO and ZnO nanoparticles.

Hence, the NCs CuO/ZnO with a ratio of (1:2:1) showed a lowest band gap energy value (2.3 eV), whereas ZnO NPs showed highest band gap energy value (2.83ev). The UV-Vis absorption peaks at 401, 375, 411, and 418 nm confirmed the synthesis of CuO, ZnO NPs, and (1:1:1) and (1:2:1) CuO/ZnO NCs, respectively. The FT-IR and different qualitative phytochemical test methods confirmed the presence of a variety of bioactive compounds alkaloids, tannins, phenols, saponins, flavonoids, terpenoids, in the *phytolacca dodecandra* leaf. The FT-IR finger print region and XRD result showed the formation of ZnO NPs, CuO NPs, and CuO/ZnO NCs.

The sizes of CuO NPs, ZnO NPs, (1:1:1), and (1:2:1) CuO/ZnO NCs was found to be 19.9, 17.1, 27.6, and 30.5 nm respectively. The synthesized NPs and NCs exhibited strong antibacterial activity for E. coli, bacteria only, while, the (1:2:1) CuO/ZnO and (1:1:1) CuO/ZnO NCs showed more antibacterial activity than CuO NPs and ZnO NPs to E. coli and salmonella, CuO/ZnO NCs exhibited a remarkably enhanced photocatalytic performance in MB dye compared to that of bare ZnO NPs. In particular, for optimized 1:2:1 ZnO/CuO NCs, about 81.5% MB degradation was achieved after 120 min of visible light irradiation. In addition, the prepared 1:2:1 CuO/ZnO NCs exhibited appreciable photocatalytic stability and reusability without significant change in their activity after three consecutive cycles. Thus, the present green-mediated (1:2:1) ZnO/CuO NC can be a promising visible-light-active photo catalyst for the removal of organic pollutants from wastewater and antibacterial activities.

5.2. Recommendation

The significant advancements in the photocatalysis of pollutants using NCs providing effective and sustainable methods for environmental remediation. Despite, CuO/ZnO NCs has efficient in MB dye degradation and antibacterial activities; there are other aspects that have not covered by this study. So, the following recommendations are provided.

- ✓ Further characterizing of synthesized NPs and NCs (SEM, BET, TGA and EDX) should be addressed utilizing additional characterization approaches not covered in this work should.
- ✓ Other microbial species should be used to examine the antimicrobial properties of CuO, ZnO NPs, and CuO/ZnO NCs.
- ✓ Synthesis of NPs and NCs using the different parts of *phytolacca dodecandra* plant other than leaves and applied for different application.

References

1. Serwecińska, L.J.W., *Antimicrobials and antibiotic-resistant bacteria: a risk to the environment and to public health.* 2020. **12**(12): p. 3313.
2. Reygaert, W.C., *An overview of the antimicrobial resistance mechanisms of bacteria.* AIMS microbiology, 2018. **4**(3): p. 482.
3. Fair, R.J. and Y. Tor, *Antibiotics and bacterial resistance in the 21st century.* Perspectives in medicinal chemistry, 2014. **6**: p. PMC. S14459.
4. Breijyeh, Z., B. Jubeh, and R. Karaman, *Resistance of gram-negative bacteria to current antibacterial agents and approaches to resolve it.* Molecules, 2020. **25**(6): p. 1340.
5. Otaibi, A.A., et al., *Sonocatalytic Degradation of Malachite Green Dye Using Green Synthesized Copper Oxide Nanoparticles.*
6. Swain, C.K.J.D.E., *Environmental pollution indices: a review on concentration of heavy metals in air, water, and soil near industrialization and urbanisation.* 2024. **2**(1): p. 5.
7. Bužga, M., et al., *Methylene blue: a controversial diagnostic acid and medication?* 2022. **11**(5): p. 711-717.
8. Alsukaibi, A.K.J.P., *Various approaches for the detoxification of toxic dyes in wastewater.* 2022. **10**(10): p. 1968.
9. Liu, H., C. Wang, and G. Wang, *Photocatalytic advanced oxidation processes for water treatment: recent advances and perspective.* Chemistry–An Asian Journal, 2020. **15**(20): p. 3239-3253.
10. Dalui, A., *Developments of Oxide Based Nano-photocatalyst in Waste Water Treatment Technology: A Brief Overview.* Back to Basics: A Multidisciplinary Approach to Organic Living and Waste Management, 2022: p. 1.
11. Albarakati, A.J. and I.A. Matter, *N-type metal oxide semiconductor: Materials and their environmental applications.* Biointerface Research in Applied Chemistry, 2023. **13**(6): p. 519.

12. Mohamed, A.A., et al., *Eco-friendly mycogenic synthesis of ZnO and CuO nanoparticles for in vitro antibacterial, antibiofilm, and antifungal applications.* Biological trace element research, 2021. **199**(7): p. 2788-2799.

13. Dejen, K.D., et al., *Green synthesis and characterisation of silver nanoparticles from leaf and bark extract of Croton macrostachyus for antibacterial activity.* Materials Technology, 2023. **38**(1): p. 2164647.

14. Ying, S., et al., *Green synthesis of nanoparticles: Current developments and limitations.* Environmental Technology & Innovation, 2022. **26**: p. 102336.

15. Bekru, A.G., et al., *Green synthesis of a CuO–ZnO nanocomposite for efficient photodegradation of methylene blue and reduction of 4-nitrophenol.* 2022. **7**(35): p. 30908-30919.

16. Liu, L., et al., *Anisotropic heavy-metal-free semiconductor nanocrystals: Synthesis, properties, and applications.* 2023. **123**(7): p. 3625-3692.

17. Bhilkar, P., et al., *Bioinspired zinc-based nanomaterials: Synthesis, biomedical, environmental and agricultural applications.* 2024. **169**: p. 81-112.

18. Chan, Y.B., et al., *Garcinia mangostana L. Leaf-Extract-Assisted Green Synthesis of CuO, ZnO and CuO-ZnO Nanomaterials for the Photocatalytic Degradation of Palm Oil Mill Effluent (POME).* 2024. **14**(8): p. 486.

19. Thatikayala, D. and B.J.J.o.M.S.M.i.E. Min, *Ginkgo leaves extract-assisted synthesis of ZnO/CuO nanocrystals for efficient UV-induced photodegradation of organic dyes and antibacterial activity.* 2021. **32**(13): p. 17154-17169.

20. Mamatha, K., et al., *Eco-inspired synthesis of ZnO/CuO nanocomposites using Phyllanthus niruri: unveiling superior photocatalytic, antibacterial efficacy against Escherichia coli and Staphylococcus aureus, and latent fingerprint studies.* 2024: p. 1-20.

21. De la Fuente, M.F., et al., *Self-medication in nonhuman primates: A systematic evaluation of the possible function of the use of medicinal plants.* American Journal of Primatology, 2022. **84**(11): p. e23438.

22. Dave, S., S. Dave, and J. Das, *Biological synthesis of platinum, palladium, copper, and zinc nanostructures*, in *Nanobiotechnology*. 2021, Elsevier. p. 211-223.

23. Raizada, A., et al., *A highly efficient copper oxide nanopowder for adsorption of methylene blue dye from aqueous medium.* Journal of Chemical Engineering Research, 2014. **2**(1): p. 249-258.

24. Szczyglewska, P., A. Feliczak-Guzik, and I. Nowak, *Nanotechnology–General Aspects: A Chemical Reduction Approach to the Synthesis of Nanoparticles.* Molecules, 2023. **28**(13): p. 4932.

25. Pandey, P., *Role of nanotechnology in electronics: A review of recent developments and patents.* Recent Patents on Nanotechnology, 2022. **16**(1): p. 45-66.

26. Shobha, G., V. Moses, and S. Ananda, *Biological synthesis of copper nanoparticles and its impact.* Int. j. pharm. sci. Invent, 2014. **3**(8): p. 6-28.

27. Khan, I., K. Saeed, and I.J.A.j.o.c. Khan, *Nanoparticles: Properties, applications and toxicities.* 2019. **12**(7): p. 908-931.

28. Xu, J., et al., *A review of the green synthesis of ZnO nanoparticles using plant extracts and their prospects for application in antibacterial textiles.* Journal of Engineered Fibers and Fabrics, 2021. **16**: p. 15589250211046242.

29. Khan, I., K. Saeed, and I. Khan, *Nanoparticles: Properties, applications and toxicities.* Arabian journal of chemistry, 2019. **12**(7): p. 908-931.

30. Ramesh, P., et al., *Green synthesis and characterization of biocompatible zinc oxide nanoparticles and evaluation of its antibacterial potential.* Sensing and Bio-Sensing Research, 2021. **31**: p. 100399.

31. Acharyulu, N., et al., *Green synthesis of CuO nanoparticles using Phyllanthus amarus leaf extract and their antibacterial activity against multidrug resistance bacteria.* Int J Eng Res Technol, 2014. **3**(4): p. pp.

32. Salem, S.S. and A. Fouda, *Green synthesis of metallic nanoparticles and their prospective biotechnological applications: an overview.* Biological trace element research, 2021. **199**: p. 344-370.

33. Gupta, M., et al., *Effective antimicrobial activity of green ZnO nano particles of Catharanthus roseus.* Frontiers in microbiology, 2018. **9**: p. 2030.

34. Kumari, S., et al., *A comprehensive review on various techniques used for synthesizing nanoparticles.* Journal of Materials Research and Technology, 2023.

35. Khan, T. and A. Mateen, *Synthesis of CuO nanoparticles by using leaf extracts of Melia azedarach and Morus nigra and their antibacterial activity.* J Innov Sci, 2018. **4**(2): p. 120.

36. Collot, M., et al., *Stealth and bright monomolecular fluorescent organic nanoparticles based on folded amphiphilic polymer.* ACS nano, 2020. **14**(10): p. 13924-13937.

37. Jeronsia, J.E., et al., *Camellia sinensis leaf extract mediated synthesis of copper oxide nanostructures for potential biomedical applications.* Materials Today: Proceedings, 2019. **8**: p. 214-222.

38. Hachem, K., et al., *Methods of chemical synthesis in the synthesis of nanomaterial and nanoparticles by the chemical deposition method: A review.* BioNanoScience, 2022. **12**(3): p. 1032-1057.

39. Islam, F., et al., *Exploring the journey of zinc oxide nanoparticles (ZnO-NPs) toward biomedical applications.* Materials, 2022. **15**(6): p. 2160.

40. Vyas, Y., et al., *Review on hydrogen production photocatalytically using carbon quantum dots: Future fuel.* 2021. **46**(75): p. 37208-37241.

41. Vijayaram, S., et al., *Applications of Green Synthesized Metal Nanoparticles—A Review.* Biological Trace Element Research, 2023: p. 1-27.

42. Pradhan, A.K., et al., *Green synthesis of silver nanoparticles from various plant extracts and its applications: A mini review.* World Journal of Biology Pharmacy and Health Sciences, 2022. **11**(1): p. 050-061.

43. El-Khawaga, A.M., A. Zidan, and A.I. Abd El-Mageed, *Preparation methods of different nanomaterials for various potential applications: A Review.* Journal of Molecular Structure, 2023. **1281**: p. 135148.

44. Tripathy, S., J. Rodrigues, and N.G. Shimpi, *Top-down and Bottom-up Approaches for Synthesis of Nanoparticles.* Nanobiomaterials: Perspectives for Medical Applications in the Diagnosis and Treatment of Diseases, 2023. **145**: p. 92-130.

45. Zhang, W.-B., et al., *Molecular nanoparticles are unique elements for macromolecular science: From "nanoatoms" to giant molecules.* Macromolecules, 2014. **47**(4): p. 1221-1239.

46. Patil, N., et al., *Overview on methods of synthesis of nanoparticles.* International Journal of Current Pharmaceutical Research, 2021. **13**(2): p. 11-16.

47. Chakraborty, N., et al., *Green synthesis of copper/copper oxide nanoparticles and their applications: a review.* Green Chemistry Letters and Reviews, 2022. **15**(1): p. 187-215.

48. Dhaka, A., et al., *A review on biological synthesis of silver nanoparticles and their potential applications.* Results in Chemistry, 2023: p. 101108.

49. Getachew, E., *Green Synthesis of CuO Nanoparticles Using Leaf Extract of Justica Schimperiana and its Antibacterial Activity*. 2020, Eskedar Getachew.

50. Leitner, W., et al., *Advanced biofuels and beyond: chemistry solutions for propulsion and production.* Angewandte Chemie International Edition, 2017. **56**(20): p. 5412-5452.

51. Nadaroglu, H., A.A. GÜNGÖR, and İ. Selvi, *Synthesis of nanoparticles by green synthesis method.* International Journal of Innovative Research and Reviews, 2017. **1**(1): p. 6-9.

52. Srivastava, S., et al., *Green synthesis of nanoparticles.* Green Nanoparticles: The Future of Nanobiotechnology, 2022: p. 53-75.

53. Ovais, M., et al., *Role of plant phytochemicals and microbial enzymes in biosynthesis of metallic nanoparticles.* 2018. **102**: p. 6799-6814.

54. Naz, S., et al., *Synthesis, biomedical applications, and toxicity of CuO nanoparticles.* Applied Microbiology and Biotechnology, 2023. **107**(4): p. 1039-1061.

55. Venkatas, J., A. Daniels, and M. Singh, *The Potential of Curcumin-Capped Nanoparticle Synthesis in Cancer Therapy: A Green Synthesis Approach.* Nanomaterials, 2022. **12**(18): p. 3201.

56. Aithal, P., *Environmental informatics: The foundation, allied & related branches—Analytical study.* International Journal of Social Sciences, 2020. **9**(1): p. 01-07.

57. Nzekekwu, A. and O. Abosede, *Green synthesis and characterization of silver nanoparticles using leaves extracts of neem (Azadirachta indica) and bitter leaf (Vernonia amygdalina).* Journal of Applied Sciences and Environmental Management, 2019. **23**(4): p. 695-699.

58. Shafey, A.M.E.J.G.P. and Synthesis, *Green synthesis of metal and metal oxide nanoparticles from plant leaf extracts and their applications: A review.* 2020. **9**(1): p. 304-339.

59. Singh, J., et al., *'Green'synthesis of metals and their oxide nanoparticles: applications for environmental remediation.* Journal of nanobiotechnology, 2018. **16**(1): p. 1-24.

60. Singh, P., et al., *Biological synthesis of nanoparticles from plants and microorganisms.* Trends in biotechnology, 2016. **34**(7): p. 588-599.

61. Jeevanandam, J., et al., *Green approaches for the synthesis of metal and metal oxide nanoparticles using microbial and plant extracts.* Nanoscale, 2022. **14**(7): p. 2534-2571.

62. Maity, D., U. Gupta, and S.J.N. Saha, *Biosynthesized metal oxide nanoparticles for sustainable agriculture: next-generation nanotechnology for crop production, protection and management.* 2022. **14**(38): p. 13950-13989.

63. Letchumanan, D., et al., *Plant-based biosynthesis of copper/copper oxide nanoparticles: An update on their applications in biomedicine, mechanisms, and toxicity.* Biomolecules, 2021. **11**(4): p. 564.

64. Shahrajabian, M.H., W. Sun, and Q. Cheng, *The importance of flavonoids and phytochemicals of medicinal plants with antiviral activities.* Mini-Reviews in Organic Chemistry, 2022. **19**(3): p. 293-318.

65. Momeni, A. and M.H. Meshkatalsadat, *Studying the Biosynthesis, Characterization, and Antibacterial Activity of Copper Oxide Nanoparticles.* International Journal of New Chemistry, 2023. **10**(3): p. 184-196.

66. Nabila, M.I. and K. Kannabiran, *Biosynthesis, characterization and antibacterial activity of copper oxide nanoparticles (CuO NPs) from actinomycetes.* Biocatalysis and agricultural biotechnology, 2018. **15**: p. 56-62.

67. Bhuvaneshwari, V., D. Vaidehi, and S. Logpriya, *Green synthesis of copper oxide nanoparticles for biological applications.* Microbiol Curr Res. 2018; 2 (1): 9-10. 10 Microbiol Curr Res. 2018 Volume 2 Issue, 2018. **1**.

68. Brhan, R., *Fabrication of Copper Oxide Nanoparticles Using Endemic Plant Lippia Adoensis: Characterization, Testing and Optimization Studies*. 2022.

69. Thate, A.G., et al., *Fabrication of TiO2-ZnO nanocomposite photoanodes to enhance the dye-sensitized solar cell efficiency.* Research on Chemical Intermediates, 2023. **49**(1): p. 147-168.

70. Palapa, N.R., et al., *CuAl LDH/Rice husk biochar composite for enhanced adsorptive removal of cationic dye from aqueous solution.* Bulletin of Chemical Reaction Engineering & Catalysis, 2020. **15**(2): p. 525-537.

71. Garg, A. and L. Chopra, *Dye Waste: A significant environmental hazard.* Materials Today: Proceedings, 2022. **48**: p. 1310-1315.

72. Kandisa, R.V., et al., *Dye removal by adsorption: a review.* Journal of bioremediation and Biodegradation, 2016. **7**(6).

73. Plakantonaki, S., et al., *A review of sustainability standards and ecolabeling in the textile industry.* Sustainability, 2023. **15**(15): p. 11589.

74. Anand, K.V., et al., *A review on the removal of dye, pesticide and pathogens from waste water using quantum dots.* European Journal of Advanced Chemistry Research, 2020. **1**(5).

75. Eldeeb, T., et al., *Adsorption of Methylene Blue (MB) dye on ozone, purified and sonicated sawdust biochars. Biomass Convers Biorefin 1–23*. 2022.

76. Eldeeb, T.M., et al., *Adsorption of methylene blue (MB) dye on ozone, purified and sonicated sawdust biochars.* Biomass Conversion and Biorefinery, 2022: p. 1-23.

77. Osorio-Aguilar, D.-M., et al., *Adsorption and Photocatalytic Degradation of Methylene Blue in Carbon Nanotubes: A Review with Bibliometric Analysis.* Catalysts, 2023. **13**(12): p. 1480.

78. Li, N., et al., *Recent developments in functional nanocomposite photocatalysts for wastewater treatment: a review.* Advanced Sustainable Systems, 2022. **6**(7): p. 2200106.

79. Twaij, B.M. and M.N. Hasan, *Bioactive secondary metabolites from plant sources: types, synthesis, and their therapeutic uses.* International Journal of Plant Biology, 2022. **13**(1): p. 4-14.

80. Sheeba Rani, M.A., *In-Vitro Anti-Diabetic Studies and In-Vitro Anti-Inflammatory Activity in an Underutilised Plant Epiphyllum oxypetalum (DC.) Hawthorn Leaves.* Bulletin of Pure & Applied Sciences-Botany, 2021(1).

81. Ozioma, E.-O.J. and O.A.N. Chinwe, *Herbal medicines in African traditional medicine.* Herbal medicine, 2019. **10**: p. 191-214.

82. Agidew, M.G., *Phytochemical analysis of some selected traditional medicinal plants in Ethiopia.* Bulletin of the National Research Centre, 2022. **46**(1): p. 87.

83. Meenakshi, K., M. Shah, and I.A. George, *Phytolacca dodecandra (African Soapberry) and Picrorhiza kurroa (Kutki)*, in *Herbs, Shrubs, and Trees of Potential Medicinal Benefits*. 2022, CRC Press. p. 203-216.

84. Debela, A.S., *Evaluation of phytoremediation potentials of Phytolacca dodecandra, Adhatoda schimperiana AND Solanum incanum FOR Selected heavy metals in field setting located in central Ethiopia*. 2020.

85. Bussmann, R.W., N.Y. Paniagua-Zambrana, and G.N. Njoroge, *Phytolacca dodecandra L'Hér. Phytolaccaceae*, in *Ethnobotany of the Mountain Regions of Africa*. 2021, Springer. p. 807-814.

86. Yemata, G., E. Yihune, and Y. Kebede, *Antibacterial Activities of Croton Macrostachyus and Pycnostachys Abyssinica Leaf Extract Isolates Against Some Human Pathogens.* Available at SSRN 4202308.

87. Gebremedhn, K., M.H. Kahsay, and M. Aklilu, *Green synthesis of CuO nanoparticles using leaf extract of Catha edulis and its antibacterial activity.* Journal of Pharmacy and Pharmacology, 2019. **7**(6): p. 327-342.

88. Abebe, H. and K. Hunie, *Phytochemical Investigation and Antibacterial Activity Assessment of Zehneria scabra (Lf) Sond (ሀረግ ፈላጊ) Leaves Extract.* Ethiopian Journal of Natural and Computational Sciences, 2022. **2**(1): p. 247-257.

89. Oakenfull, D. and G.S. Sidhu, *Saponins.* Toxicants of plant origin, 2023: p. 97-142.

90. Veeramanikandan, V., et al., *Green synthesis, characterization of iron oxide nanoparticles using Leucas aspera leaf extract and evaluation of antibacterial and antioxidant studies.* International Journal of Agriculture Innovations and Research, 2017. **6**(02): p. 242-250.

91. Getu, Z. and M. Aklilu, *Biosynthesis of silver nanoparticles using Endod (Phytolacca dodecandra) leaf extract and evaluation of their antibacterial activity.* Ethiopian Journal of Science and Technology, 2023. **16**(1): p. 77-97.

92. Andualem, W.W., et al., *Synthesis of copper oxide nanoparticles using plant leaf extract of Catha edulis and its antibacterial activity.* Journal of Nanotechnology, 2020. **2020**: p. 1-10.

93. Murugan, B., et al., *Green synthesis of CuO nanoparticles for biological applications.* Inorganic Chemistry Communications, 2023: p. 111088.

94. Takele, E., et al., *Green synthesis, characterization, and antibacterial activity of CuO/ZnO nanocomposite using Zingiber officinale Rhizome Extract.* 2023. **2023**(1): p. 3481389.

95. Widatalla, H.A., et al., *Green synthesis of silver nanoparticles using green tea leaf extract, characterization and evaluation of antimicrobial activity.* Nanoscale Advances, 2022. **4**(3): p. 911-915.

96. Kumar, M.A., et al., *Evaluation of bi-functional applications of ZnO nanoparticles prepared by green and chemical methods.* Journal of Environmental Chemical Engineering, 2019. **7**(6): p. 103468.

97. Sharmila, G., M. Thirumarimurugan, and C. Muthukumaran, *Green synthesis of ZnO nanoparticles using Tecoma castanifolia leaf extract: Characterization and evaluation of its antioxidant, bactericidal and anticancer activities.* Microchemical Journal, 2019. **145**: p. 578-587.

98. Ghareib, M., et al., *Biosynthesis of copper oxide nanoparticles using the preformed biomass of aspergillus fumigatus and their antibacterial and photocatalytic activities.* Digest Journal of Nanomaterials & Biostructures (DJNB), 2019. **14**(2).

99. Alkaykh, S., A. Mbarek, and E.E. Ali-Shattle, *Photocatalytic degradation of methylene blue dye in aqueous solution by MnTiO3 nanoparticles under sunlight irradiation.* Heliyon, 2020. **6**(4).

100. Jalali, N., et al., *Photocatalytic properties of ZnO/CuO nanocomposite prepared in acidic media.* 2022. **55**(1): p. 21-30.

101. Ahmaruzzaman, M.J.N.f.E.E., *Metal oxides (ZnO, CuO and NiO)-based nanostructured materials for photocatalytic remediation of organic contaminants.* 2023. **8**(1): p. 219-235.

102. Gosa, B.B. and T.W.J.I.J.E.A.B. Wana, *Evaluation of the phytochemical and antibacterial activity of four selected plant extracts against some pathogenic bacteria.* 2022. **7**(4): p. 265-276.

103. Khan, S., et al., *Optimization of process parameters for the synthesis of silver nanoparticles from Piper betle leaf aqueous extract, and evaluation of their antiphytofungal activity.* 2020. **27**: p. 27221-27233.

104. Gebremedhn, K., et al., *Green synthesis of CuO nanoparticles using leaf extract of Catha edulis and its antibacterial activity.* 2019. **7**(6): p. 2328-2150.

105. Prema, P., et al., *Statistical optimization of silver nanoparticle synthesis by green tea extract and its efficacy on colorimetric detection of mercury from industrial waste water.* 2022. **204**: p. 111915.

106. Habibullah, G., J. Viktorova, and T.J.N.R.L. Ruml, *C urrent strategies for noble metal nanoparticle synthesis.* 2021. **16**(1): p. 47.

107. Zelekew, O.A., et al., *Recent progress on plant extract-mediated biosynthesis of ZnO-based nanocatalysts for environmental remediation: Challenges and future outlooks.* 2023. **317**: p. 102931.

108. Fang, H.-B., et al., *Fragmented phosphorus-doped graphitic carbon nitride nanoflakes with broad sub-bandgap absorption for highly efficient visible-light photocatalytic hydrogen evolution.* 2018. **225**: p. 397-405.

109. Shaik, M.R., et al., *Plant-extract-assisted green synthesis of silver nanoparticles using Origanum vulgare L. extract and their microbicidal activities.* 2018. **10**(4): p. 913.

110. Donia, D., M.J.I.j.o.e.s. Carbone, and technology, *Fate of the nanoparticles in environmental cycles.* 2019. **16**: p. 583-600.

111. Ali, A., et al., *Synthesis, characterization, applications, and challenges of iron oxide nanoparticles.* 2016: p. 49-67.

112. Mabrouk, M., et al., *Nanomaterials for biomedical applications: production, characterisations, recent trends and difficulties.* 2021. **26**(4): p. 1077.

113. Mamo, G.M. and S.Y.J.R.i.C. Ejeta, *Copper Oxide-Nickel oxide nanocomposites synthesized via Allium cepa peel extract for photocatalytic degradation of methylene blue.* 2024. **11**: p. 101801.

114. Li, J., C.Y. Huang, and C.J.J.A.C. Li, *Deoxygenative functionalizations of aldehydes, ketones and carboxylic acids.* 2022. **134**(10): p. e202112770.

115. Negash, Y., et al., *Antibacterial Activites of the CuO/ZnO Nanocomposite Grown on Silica Extracting from Bagasse Ash.* 2021. **8**(1): p. 65-72.

116. Endeshaw, S.B., et al., *Croton macrostachyus Leaf Extract-Mediated Green Synthesis of ZnO Nanoparticles and ZnO/CuO Nanocomposites for the Enhanced Photodegradation of Methylene Blue Dye with the COMSOL Simulation Model.* 2023. **9**(1): p. 559-572.

117. Raya, I., et al., *RETRACTED: Synthesis, Characterization and Photodegradation Studies of Copper Oxide–Graphene Nanocomposites.* 2021. **11**(12): p. 1452.

118. Saravanakkumar, D., et al., *Synthesis and characterization of ZnO–CuO nanocomposites powder by modified perfume spray pyrolysis method and its antimicrobial investigation.* 2018. **39**(3): p. 033001.

119. Sudharshan, N. and V. Swetha, *Uv-visible spectroscopy: a comprehensive review on instrumentation.* 2023.

120. Yadeta Gemachu, L., A.J.G.C.L. Lealem Birhanu, and Reviews, *Green synthesis of ZnO, CuO and NiO nanoparticles using Neem leaf extract and comparing their photocatalytic activity under solar irradiation.* 2024. **17**(1): p. 2293841.

121. Meena, P.L., et al., *Fabrication of ZnO/CuO hybrid nanocomposite for photocatalytic degradation of brilliant cresyl blue (BCB) dye in aqueous solutions.* 2021. **6**(3): p. 196-211.

122. Sidiqi, U., et al., *Progress on cupric oxide based nanomaterials: Exploring advancements in their synthesis, applications and prospects.* 2024. **308**: p. 117598.

123. Shinde, R.S., et al., *Synthesis and characterization of ZnO/CuO nanocomposites as an effective photocatalyst and gas sensor for environmental remediation.* 2022: p. 1-22.

124. Liu, G., et al., *A red anatase TiO 2 photocatalyst for solar energy conversion.* 2012. **5**(11): p. 9603-9610.

125. Stanić, V. and S.B. Tanasković, *Antibacterial activity of metal oxide nanoparticles,* in *Nanotoxicity*. 2020, Elsevier. p. 241-274.

126. Sapkota, K.P., et al., *Coherent CuO-ZnO nanobullets maneuvered for photocatalytic hydrogen generation and degradation of a persistent water pollutant under visible-light illumination.* 2021. **9**(6): p. 106497.

127. Cui, L., et al., *In situ study of the antibacterial activity and mechanism of action of silver nanoparticles by surface-enhanced Raman spectroscopy.* 2013. **85**(11): p. 5436-5443.

128. Altun, E., et al., *Metal-based nanoparticles for combating antibiotic resistance.* 2021. **8**(4).

129. Song, Z., et al., *Synergistic antibacterial effects of curcumin modified silver nanoparticles through ROS-mediated pathways.* 2019. **99**: p. 255-263.

130. Zhang, Q., et al., *Preparation of highly efficient and magnetically recyclable Fe3O4@ C@ Ru nanocomposite for the photocatalytic degradation of methylene blue in visible light.* 2019. **483**: p. 241-251.

131. Das, S. and V.C.J.N.R. Srivastava, *An overview of the synthesis of CuO-ZnO nanocomposite for environmental and other applications.* 2018. **7**(3): p. 267-282.

132. Samadi, M., et al., *Recent progress on doped ZnO nanostructures for visible-light photocatalysis.* 2016. **605**: p. 2-19.

133. Chanu, L.A., et al., *Effect of operational parameters on the photocatalytic degradation of Methylene blue dye solution using manganese doped ZnO nanoparticles.* 2019. **12**: p. 1230-1237.

134. Pradhan, A.C., et al., *Fabrication of the mesoporous Fe@ MnO2NPs–MCM-41 nanocomposite: an efficient photocatalyst for rapid degradation of phenolic compounds.* 2015. **119**(25): p. 14145-14159.

135. Chakraborty, A., D.A. Islam, and H.J.M.R.B. Acharya, *One pot synthesis of ZnO-CuO nanocomposites for catalytic peroxidase like activity and dye degradation.* 2019. **120**: p. 110592.

136. Waghchaure, R.H., V.A. Adole, and B.S.J.I.C.C. Jagdale, *Photocatalytic degradation of methylene blue, rhodamine B, methyl orange and Eriochrome black T dyes by modified ZnO nanocatalysts: A concise review.* 2022. **143**: p. 109764.

137. Haleem, A., et al., *A comprehensive review on adsorption, photocatalytic and chemical degradation of dyes and nitro-compounds over different kinds of porous and composite materials.* 2023. **28**(3): p. 1081.

138. Hien, N., et al., *Heterogeneous catalyst ozonation of Direct Black 22 from aqueous solution in the presence of metal slags originating from industrial solid wastes.* 2020. **233**: p. 115961.

139. Karim, A.V. and A.J.C.E.J. Shriwastav, *Degradation of ciprofloxacin using photo, sono, and sonophotocatalytic oxidation with visible light and low-frequency ultrasound: Degradation kinetics and pathways.* 2020. **392**: p. 124853.

140. Ma, Z., et al., *Highlighting unique function of immobilized superoxide on TiO2 for selective photocatalytic degradation.* 2020. **238**: p. 116402.

141. Le Pham, H.A., et al., *Optimization of photocatalytic degradation performance of organic dye using highly efficient bismuth MOFs: Preparation and parametric analysis.* 2023. **198**: p. 196-207.

142. Kumari, V., et al., *Hydrothermal synthesis conditions effect on hierarchical ZnO/CuO hybrid materials and their photocatalytic activity.* 2021. **32**: p. 9596-9610.

143. Barman, D., et al., *Design strategy for CuO-ZnO S-scheme heterojunction photocatalysts in the presence of plasmonic Ag and insights into photoexcited carrier generation and interfacial transfer in diverse structural configurations of the heterostructure system.* 2023. **663**: p. 131077.

144. Siddiqui, V.U., et al., *Optimization of facile synthesized ZnO/CuO nanophotocatalyst for organic dye degradation by visible light irradiation using response surface methodology.* 2021. **11**(12): p. 1509.

145. Oliveira, M.C., et al., *DFT Simulations for Heterogeneous Photocatalysis from ZnO and CuO Semiconductors*, in *Functional Properties of Advanced Engineering Materials and Biomolecules*. 2021, Springer. p. 185-200.

146. Yadav, G., et al., *A comprehensive review on low-cost waste-derived catalysts for environmental remediation.* 2023. **164**: p. 112261.

147. Zeghdi, S., et al., *Improved Synthesis of Cu2O NPs and Ascorbic Acid-Modified Derivatives for Adsorption of Brilliant Cresyl Blue: Surface and Reusability Studies.* 2024. **17**(10): p. 2358.

148. Lanjwani, M.F., et al., *Trends in photocatalytic degradation of organic dye pollutants using nanoparticles: a review.* 2024. **159**: p. 111613.

Appendix

A. Optimization of Precursor Metal Salt Concentration

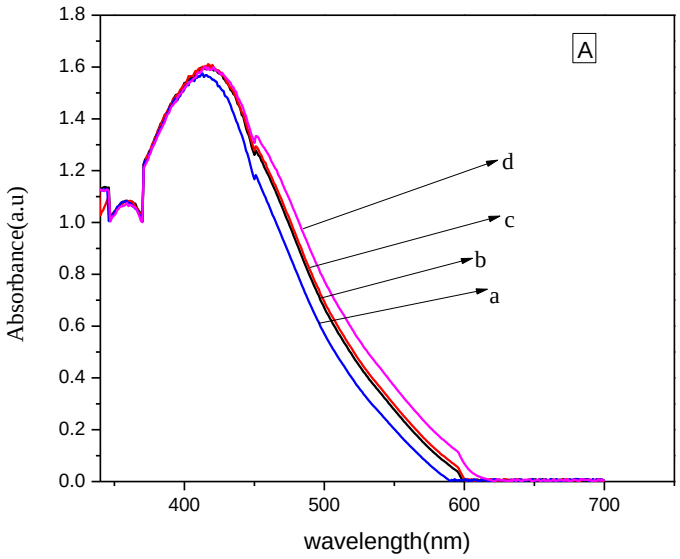

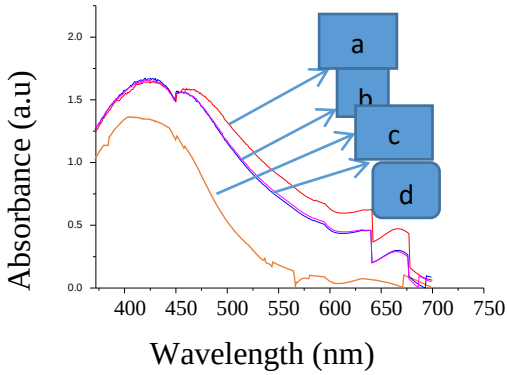

B.

Figure 18.The UV-Vis spectra of ZnO (A) at pH = 9 formed using 4% of leaf extract and (a) 0.06M (b) 0.08 (c) 0.1M (d) 0.12M of $ZnSO_4.7H_2O$ and CuO (B) at pH = 10 NPs formed using (a) 0.12M (b) 0.08M (c) 0.06M (d) 0.1M of $CuSO_4.5H_2O$.

B. Optimization of Plant Concentration of *phytolacca dodecandra* leaf extract

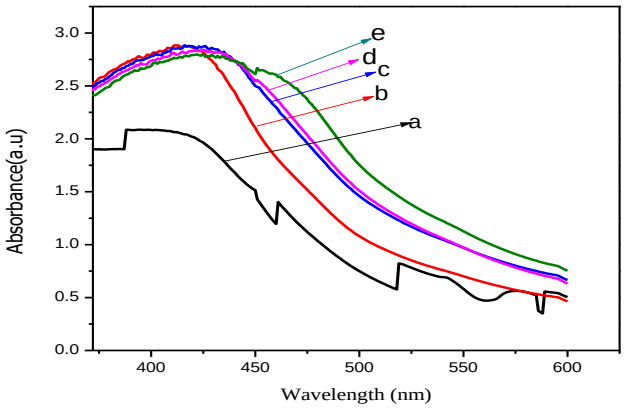

Figure 19. The UV-Vis spectra of NPs formed using 40 mL of 0.1M of Cu and Zn precursor and (a) 3% (b) 4% (c) 5% (d) 6% (e) 7% leaf extract of phytolacca dodecandra pH = 10 and 9

C. Optimization of volume ratio of precursor and plant

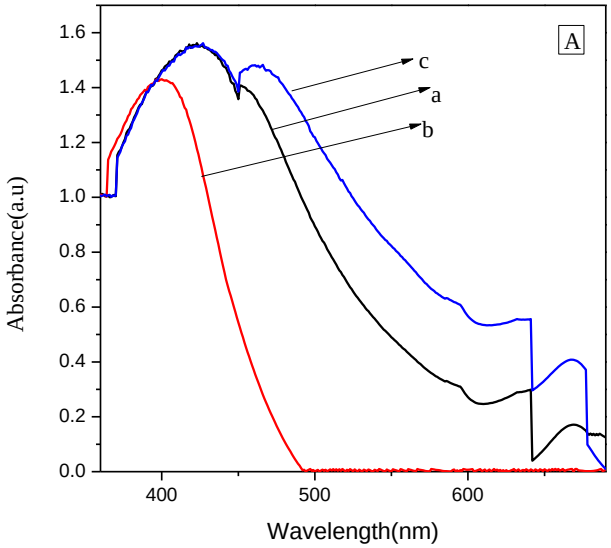

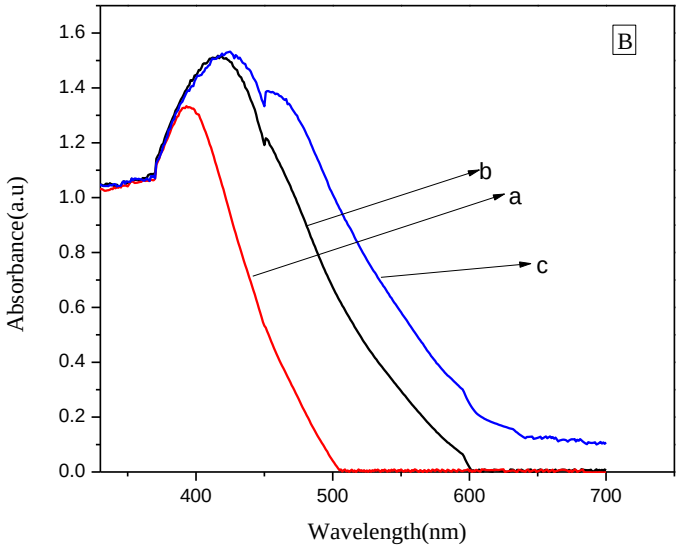

Figure 20. The Uv-visible spectra of CuO(A) at pH = 10 and ZnO (B) at pH = 9NPs formed using 4% of leaf powder , 0.1M of Cu and Zn precursor and (a) 2:1 (b) 1:1 (c) 1:2,ratio of leaf extract of phytolacca dodecandra and precursors.

D. Optimization of pH of the mixture of precursor and plant extract

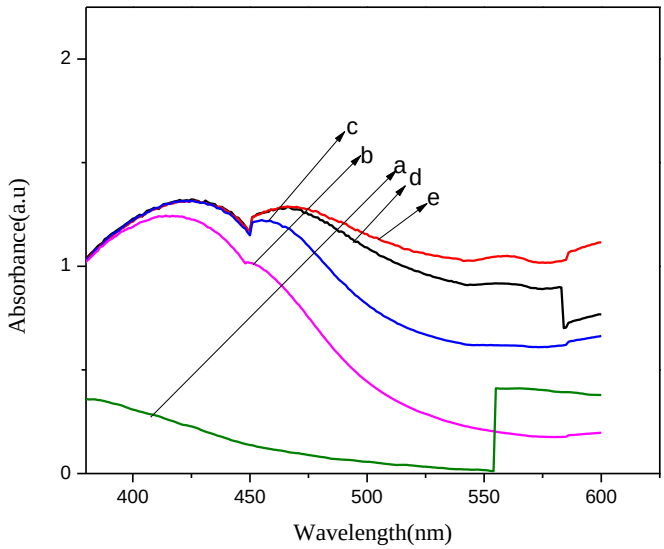

A.

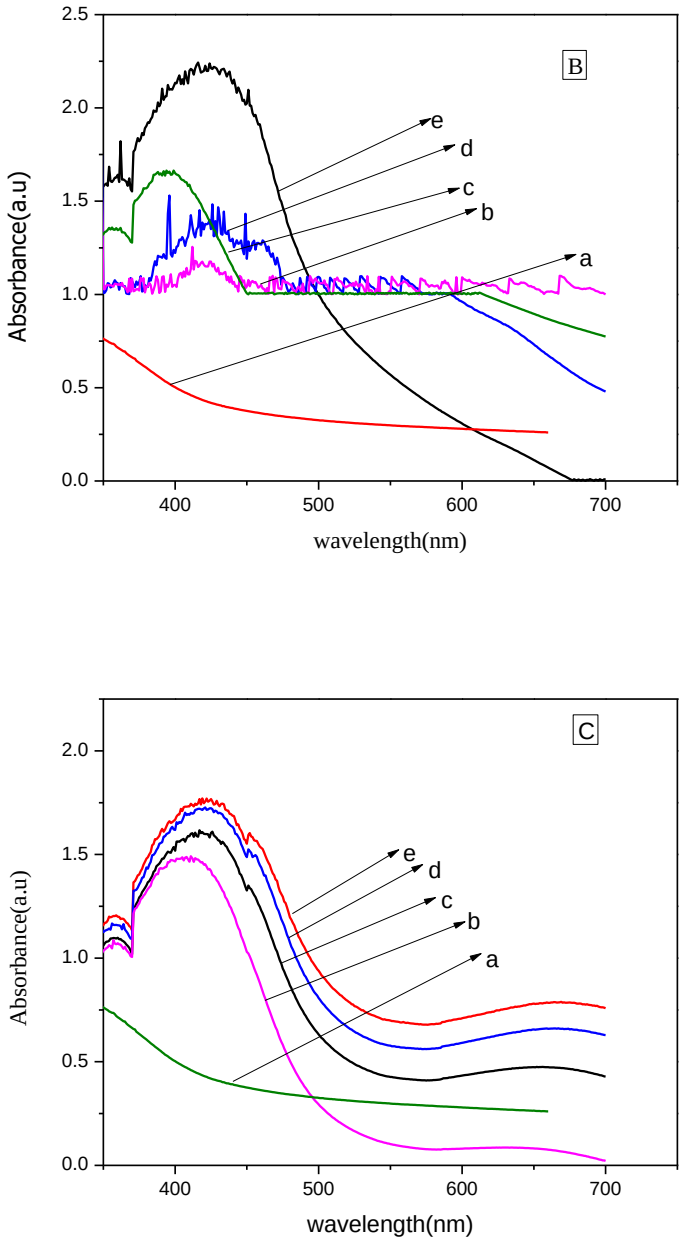

Figure 21. The UV-Vis spectra of CuO(A), ZnO(B) NPs and CuO/ZnO(C) NCs formed using 4% of leaf powder, 0.1M of precursor 1:1NPs, and 1:1:1,1:2:1 CuO/ZnO NCs ratio and (a) 12 (b) 11 (c) 10 (d) 8 (e) 9

E. Optimization of Reaction Time

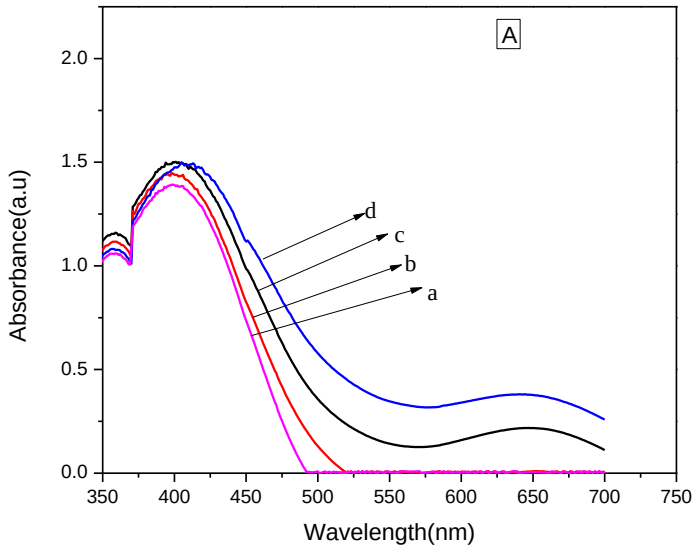

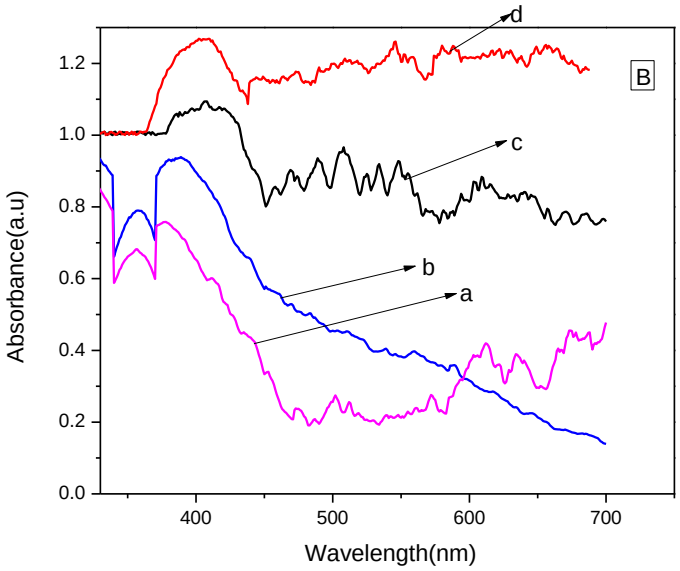

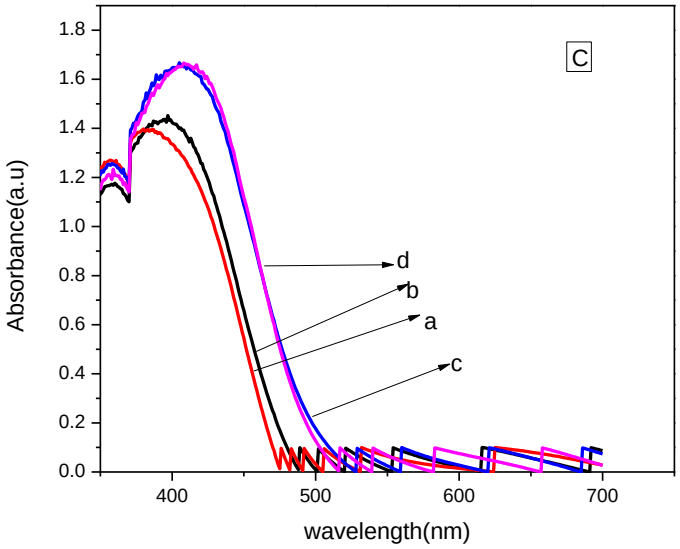

Figure 22.The UV-Vis spectra of CuO(A) NPs at pH = 10,(1:1)v/v ratio formed using (a) 120min (b) 60min (c) 90min (d) 30min, ZnO(B) NPs at pH = 9,(1:1)v/v ratio formed using (a) 120min (b) 90min (c) 30min (d) 60min and CuO/ZnO(C) at pH = 10, (1:1:1) and (1:2:1)v/v ratio NCs formed using and (a) 30min (b) 120min (c) 60min (d) 90min of 4% leaf extract of *phytolacca dodecandra* and 0.1M precursors.

Table 7. Optimization of parameters, their amounts for synthesis of nanoparticles and optimum value.

No.	Optimize parameters	Dose range	pH	Precursor(M)	*Phytolacadodecandra* (w/v)	℃	Contact time(min)	Ratio(v/v)	Optimal value
1	Precursor metal salt	(0.06-0.12)M	9		4	80	30	1:1,1:1:1,1:2:1	0.1M
2	*Phytolacca dodecandra* leaf extract	2-7% w/v	9	0.1	2-7	80	30	>>	4%w/v
3	Volume ratio of precursor and plant	1:1,1:2,2:1v/v 1:1:1,1:2:1,2:1:1v/v	9	0.1	4	80	30		1:1v/v, 1:1:1, 12:1v/v volume ratio
4	pH	2-12		0.1	4	80	30	>>	9 and 10
5	Temperature	25-90℃	9& 10	0.1	4		30	>>	70℃
6	Reaction Time	30-120min	9& 10	0.1	4	70		>>	90min

Table 8. Optimization parameters and %degradation

No.	Parameters	Dose rang	NPs &NCs	pH	MB (ppm)	Time(min)	Degradation efficiency of NPs &NCs	Optimum value
1	pH	2-12	20 mg		10	20	ZnO NPs(30, 32, 38, 43, 54, 53, 52) % CuO NPs (28, 30.5, 38, 40, 55, 52.6, 51,49.5) % 1:1:1CuO/ZnO (31,38, 41, 50, 65, 64, 62)% 1:2:1CuO/ZnO(36,39,48, 58, 74, 72, 69)%	pH=10
2	Dosage NPs & NCs	(10-60) mg		10	10	20	ZnO (35, 37, 47, 54, 52, 51,49)% CuO(38,40.3,53,55,54,54,53)%,1:1:1CuO/ZnO(37,45,56,65,63.4,63)% 1:2:1CuO/ZnO(37,45, 56, 65, 63.4, 63)%	ZnO (30mg)&40mg
3	MB dose(ppm)	(10-36)ppm	30 &40	10		20	ZnO NPs(60,57.5,56,49.5,46,42)% CuONPs(65.5,63,59.2,55,53,47.5)% 1:1:1CuO/ZnO(74,72.3,68.5,65.6,60,55.3)% 1:2:1CuO/ZnO(77,75,73.2,69,63,59)%	10ppm
4	Contact	(20-140)	30 &4	10	10	120	ZnONPs(47,52,57,59.5,60,66,64)%	120min

	time	min	0				CuONPs(51,54.5,58,60,62.3,68,65.5)% 1:1:1CuO/ZnO(55,57.3,60,63,66.5,77,75.5)% 1:2:1CuO/ZnO-57,60,62.5,68,76,81.7,80)%	

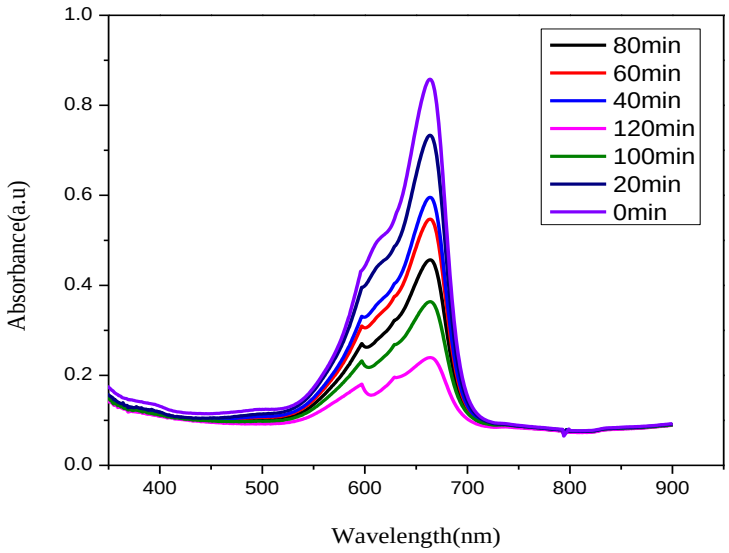

A

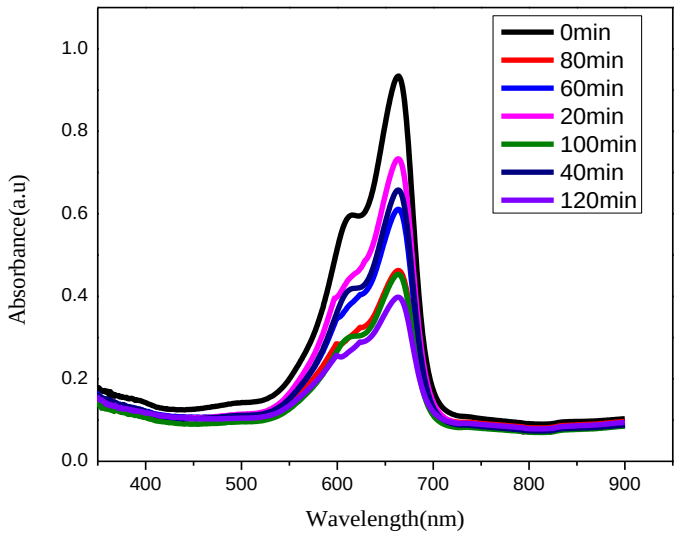

B

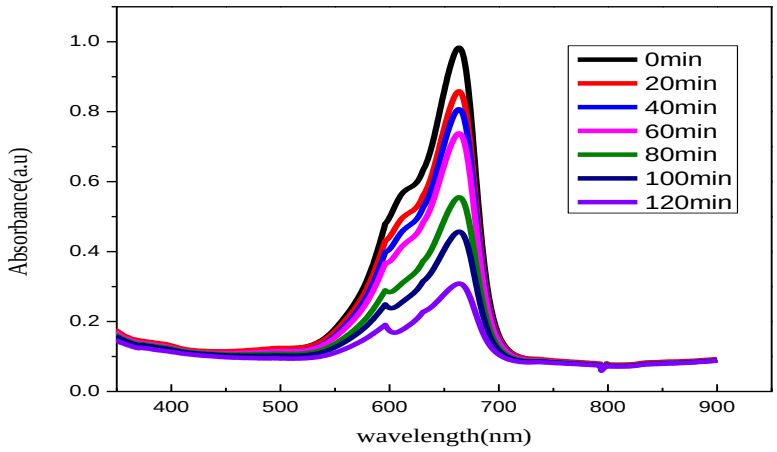

C.

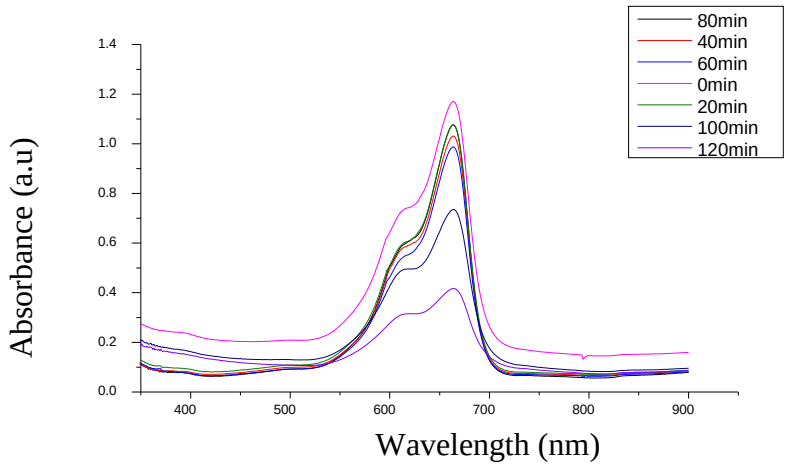

D.

Figure 23. UV–Visible spectra showing the reduction in the intensity of MB solution under sun light irradiation by using (a) 1:2:1CuO/ZnO NCs (b) ZnO NPs (c) 1:1: 1 CuO/ZnO NCs (d) CuO NPs